

**ANALYSIS OF HEAT TRANSFER AND THERMAL STABILITY IN A SLAB
SUBJECTED TO ARRHENIUS KINETICS**

by

ANNAH MOKGANYETJI KGOTLELELO LEGODI

[BSc., BSc.(Hons) – UL South Africa]

Thesis submitted in fulfillment of the requirements for the degree

Master of Technology: Mechanical Engineering

Cape Peninsula University of Technology

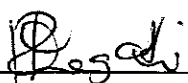
Supervisor: Prof. O.D. Makinde

Bellville, South Africa

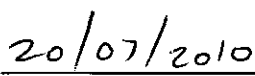
May 2010

DECLARATION

I, Annah Mokganyetji Kgotlelelo Legodi, hereby declare that, this thesis represents my own work and has not been submitted previously for examination towards any degree or diploma qualification at any other University. Further more it represents my own opinions and not necessarily those of the Cape Peninsula University of Technology.



Signed



Date

ABSTRACT

Development of safe storage for reactive combustible materials to prevent possible human and environmental hazards as well as ensure and enhance industrial safety can significantly benefit from mathematical modelling of systems. In the recent past, models with varying degrees of sophistication have been developed and applied to the problem of predicting thermal criticality conditions, temperature and concentration profiles of such system.

In this thesis, a model showing the temperature history of an n th order exothermic oxidation reaction in a slab of combustible material with variable pre-exponential factor, taking the consumption of the reactant into account in the presence of a convective heating and oxygen exchange at the slab surface with the ambient is presented. Both transient and steady state problems are tackled. The critical regime separating the regions of explosive and non-explosive paths of a one step exothermic chemical reaction is determined. The governing nonlinear partial differential equations are solved numerically by method of lines (MOL), with finite difference schemes used for the discretisation of the spatial derivatives. Moreover, both fourth order Runge-Kutta numerical integration coupled with shooting methods and perturbation techniques together with a special type of Hermite-Padé series summation and improvement method were employed to tackle the steady state problem. The crucial roles played by the boundary conditions in determining the location of the maximum heating were demonstrated.

In chapter one, the relevant applications together with previous published work on the problem were highlighted. The basic mathematical theory and equations needed to tackle the problem were derived in Chapter two. In chapter three, the transient model problem was formulated, analysed and discussed. The steady state problem was formulated and solved in Chapter four. Furtherwork and concluding remarks were highlighted in Chapter five.

Acknowledgements

I would like to thank God for His love and protection, for bringing me this far and all the blessings He is giving me.

Prof. O.D. Makinde, my supervisor, for his dedication and support.

National Research Foundation (NRF) for their financial assistance.

A special word of thanks to my husband Matsatse for his unchanging love and support.

I also acknowledge my two families, Kgasago's and Legodi's, for their support, encouragement and prayers.

DEDICATION

To my parents Hlabanteke and Ramatsimele Kgasago , my mothers in-law Sinah Pale and Jeminah Legodi, my husband Matsatse and our children Kholofelo and Kagisho .

TABLE OF CONTENTS

| | |
|--|------|
| DECLARATION | ii |
| ABSTRACT | iii |
| ACKNOWLEDGEMENTS | iv |
| DEDICATION | v |
| LIST OF FIGURES | viii |
| LIST OF TABLES | x |
| NOMENCLATURE | xi |
| CHAPTER 1 | 1 |
| Introduction | 1 |
| 1.1 Definition of terms | 3 |
| 1.2 Statement of the problem | 8 |
| 1.3 Objectives of the Study | 9 |
| 1.4 Significance of the Study | 9 |
| 1.5 Research Hypotheses | 9 |
| 1.6 Methodology | 10 |
| CHAPTER 2 | 11 |
| Derivation of basic equations for the problem | 11 |
| 2.1 Energy Equation | 11 |
| 2.1.1 The Zeroth Law of Thermodynamics | 11 |
| 2.1.2 The First Law of Thermodynamics | 11 |
| 2.1.3 Fourier Conduction | 13 |
| 2.2 Concentration Equation | 15 |
| CHAPTER 3 | 22 |
| 3.1 Transient heating of slab under an n^{th} order oxidation chemical reaction | 18 |
| 3.1.1 Summary | 18 |
| 3.1.2 Introduction | 18 |
| 3.1.3 Mathematical model | 20 |
| 3.1.4 Numerical procedure | 22 |
| 3.1.5 Results and Discussion | 22 |
| 3.1.6 Conclusion | 33 |
| CHAPTER 4 | 34 |
| 4.1 Analysis of steady state exothermic reaction in a slab with convective boundary conditions | 34 |

| | |
|--|-----------|
| 4.1.1 Summary | 34 |
| 4.1.2 Introduction | 34 |
| 4.1.3 Mathematical model | 35 |
| 4.1.4 Perturbation Method | 37 |
| 4.1.5 Hermite - Padé approximation Technique | 39 |
| 4.1.6 Numerical approach | 40 |
| 4.1.7 Results and Discussion | 40 |
| CHAPTER 5 | 53 |
| 5.1 Conclusion | 53 |
| 5.2 Further Work | 54 |
| References | 55 |

LIST OF FIGURES

| | |
|---|----|
| Figure 1.01: A sketch of an exothermic reaction | 5 |
| Figure 1.02: Picture showing the explosions of materials under strong exothermic reactions | 5 |
| Figure 2.2.01: Change in Mass flux in a given volume | 15 |
| Figure 2.2.02: Change in Mass flux in a given volume | 16 |
| Figure 3.1.3.1: Geometry of the Problem | 20 |
| Figure 3.1.5.2. Temperature profiles for $m=0.5, n=2, \alpha=\beta=\lambda=\gamma=Bi=1, \theta_a=\varepsilon=0.1$ | 24 |
| Figure 3.1.5.3. Three dimensional plot for temperature profiles for $m=0.5, n=2, \alpha=\beta=\lambda=\gamma=Bi=1, \theta_a=\varepsilon=0.1$ | 25 |
| Figure 3.1.5.4. Temperature profiles for $t=10, n=2, \alpha=\beta=\lambda=\gamma=Bi=1, \theta_a=\varepsilon=0.1$ | 25 |
| Figure 3.1.5.5. Temperature profiles for $t=10, m=0.5, \alpha=\beta=\lambda=\gamma=Bi=1, \theta_a=\varepsilon=0.1$ | 26 |
| Figure 3.1.5.6. Temperature profiles for $t=10, m=0.5, n=2, \alpha=\beta=\lambda=\gamma=1, \theta_a=\varepsilon=0.1$ | 26 |
| Figure 3.1.5.7. Temperature profiles for $t=10, m=0.5, n=2, \alpha=\gamma=\lambda=Bi=1, \theta_a=\varepsilon=0.1$ | 27 |
| Figure 3.1.5.8. Temperature profiles for $t=10, n=2, m=0.5, \alpha=\beta=\gamma=Bi=1, \theta_a=\varepsilon=0.1$ | 27 |
| Figure 3.1.5.9. Temperature profiles for $t=10, m=0.5, n=2, \alpha=\beta=\lambda=Bi=1, \theta_a=\varepsilon=0.1$ | 28 |
| Figure 3.1.5.10. Oxygen concentration profiles for $m=0.5, n=2, \alpha=\beta=\lambda=\gamma=Bi=1, \theta_a=\varepsilon=0.1$ | 29 |
| Figure 3.1.5.11. Three dimensional plot for Oxygen concentration profiles for $m=0.5, n=2, \alpha=\beta=\lambda=\gamma=Bi=1, \theta_a=\varepsilon=0.1$ | 30 |
| Figure 3.1.5.12. Oxygen concentration profiles for $t=10, n=2, \alpha=\beta=\lambda=\gamma=Bi=1, \theta_a=\varepsilon=0.1$ | 30 |

| | |
|--|----|
| Figure 3.1.5.13. Oxygen concentration profiles for $t=10, m=0.5,$ $\alpha=\beta=\lambda=\gamma=Bi=1, \theta_a=\varepsilon=0.1$ | 31 |
| Figure 3.1.5.14. Oxygen concentration profiles for $t=10, m=0.5, n=2,$ $\alpha=\beta=\lambda=\gamma=1, \theta_a=\varepsilon=0.1$ | 31 |
| Figure 3.1.5.15. Oxygen concentration profiles for $t=10, m=0.5, n=2,$ $\alpha=\beta=\lambda=Bi=1, \theta_a=\varepsilon=0.1$ | 32 |
| Figure 3.1.5.16. Oxygen concentration profiles for $t=10, n=2, m=0.5,$ $\alpha=\beta=\gamma=Bi=1, \theta_a=\varepsilon=0.1$ | 32 |
| Figure 3.1.5.17. Oxygen concentration profiles for $t=10, m=0.5, n=2,$ $\alpha=\gamma=\lambda=Bi=1, \theta_a=\varepsilon=0.1$ | 33 |
| Figure 4.1.3.1: Geometry of the Problem | 36 |
| Figure 4.1.7.1. A slice of approximate bifurcation diagram in the (λ, θ_{max}) plane when $\beta =$ $0.1, \varepsilon=0, \gamma=Bi=\theta_a=n=1.$ | 44 |
| Figure 4.1.7.2. Temperature profiles for $n=2, \beta=\lambda=\gamma=Bi=\theta_a=1, \varepsilon=0.1$ | 45 |
| Figure 4.1.7.3. Temperature profiles for $m=0.5, \beta=\lambda=\gamma=Bi=\theta_a=1, \varepsilon=0.1$ | 46 |
| Figure 4.1.7.4. Temperature profiles for $n=2, m=0.5, \beta=\lambda=\gamma=\theta_a=1, \varepsilon=0.1$ | 46 |
| Figure 4.1.7.5. Temperature profiles for $n=2, m=0.5, \lambda=Bi=\gamma=\theta_a=1, \varepsilon=0.1$ | 47 |
| Figure 4.1.7.6. Temperature profiles for $n=2, m=0.5, \beta=Bi=\gamma=\theta_a=1, \varepsilon=0.1$ | 47 |
| Figure 4.1.7.7. Temperature profiles for $n=2, m=0.5, \beta=Bi=\lambda=\theta_a=1, \varepsilon=0.$ | 48 |
| Figure 4.1.7.8. Oxygen concentration profiles for $n=2, \beta=\lambda=\gamma=Bi=\theta_a=1, \varepsilon=0.1$ | 49 |
| Figure 4.1.7.9. Oxygen concentration profiles for $m=0.5, \beta=\lambda=\gamma=Bi=\theta_a=1, \varepsilon=0.1$ | 50 |
| Figure 4.1.7.10. Oxygen concentration profiles for $n=2, m=0.5, \beta=\lambda=\gamma=\theta_a=1,$ $\varepsilon=0.1$ | 50 |
| Figure 4.1.7.11. Oxygen concentration profiles for $n=2, m=0.5, \beta=Bi=\lambda=\theta_a=1, \varepsilon$ $=0.1$ | 51 |
| Figure 4.1.7.12. Oxygen concentration profiles for $n=2, m=0.5, \beta=Bi=\gamma=\theta_a=1, \varepsilon$ $=0.1$ | 51 |
| Figure 4.1.7.13. Oxygen concentration profiles for $n=2, m=0.5, \lambda=Bi=\gamma=\theta_a=1,$ $\varepsilon=0.1$ | 52 |

LIST OF TABLES

| | |
|--|----|
| Table 4.1.7.1: Comparison between analytical and numerical results ($\lambda=\beta=\gamma=0.1$, $\varepsilon=0$, $n=2$, $Bi=\theta_a=1$) | 41 |
| Table 4.1.7.2: Computations showing the criticality procedure rapid convergence ($\beta=0.1$, $\gamma=Bi=\theta_a=n=1$, $\varepsilon=0$) | 41 |
| Table 4.1.7.3: Computations showing thermal ignition criticality for different parameter values | 42 |

| Symbol | NOMENCLATURE Description |
|---------------|--|
| ρ | Density |
| K | Thermal Conductivity |
| T | Absolute Temperature |
| T_a | Ambient Temperature |
| T_0 | Initial Temperature |
| t | Time |
| Q | Exothermicity |
| c_p | Specific Heat at a Constant pressure |
| C_a | Ambient Oxygen concentration |
| C_0 | Initial Oxygen concentration in the material |
| γ | Oxygen transfer parameter |
| β | Oxygen consumption rate |
| B_i | Biot number |
| λ | Frank kamenetski parameter |

1. INTRODUCTION

When cellulosic materials such as cotton, hay, sawdust or bagasse (sugar-cane residue) are stored in sufficient large quantities they may self-heat with the possibility of spontaneous ignition. Self-heating is a process where a material increases in temperature due to the release of heat from ongoing chemical reactions and without drawing heat from its surroundings. The conditions which determine whether self-heating may lead to spontaneous ignition include the rate of internal heat generation and the body's insulation properties, i.e. the rate of air supply and heat release. Spontaneous ignition is a major concern because of the dangers associated with fires and the associated destruction or spoilage of the stored product. While ignition characteristics or criticality for a given stored material depend on a combination of properties including ambient temperature, surface characteristics and the chemistry of the material itself, the geometry is particularly relevant with regard to questions of physical storage. When all other properties are unchanged a small body will lose heat far more rapidly than a large body of the same material, with the surface /volume ratio playing a crucial role in defining criticality.

Mathematical models of heat transfer and thermal stability in a slab usually involve nonlinear terms in the equations for energy and mass conservation. The nonlinearities in the energy and mass equations tend to preclude its exact analytical solutions, although it is sometimes possible to construct asymptotic solutions for certain parameter ranges. The pioneering works on the basic theory of thermal explosion was developed by Semenov [1] and Frank-Kamenetskii [2]. Thereafter, several authors have generalized the idea with respect to various engineering and industrial applications they include [3], [4], [5], and [6]. Perhaps the formulation required can be most readily understood if one considers a large flat slab having thermal properties independent of direction within the material. The average temperature rise in a given time multiplied by the amount of heat stored in the time will equal the difference between the heat that flowed in and that which flowed out during the given time. Moreover, in a slab the following heat sources can lead to heat generation;

- A heat production rate, deriving from Arrhenius type oxidation reactions inside the slab.
- A physical heat production/consumption rate, which reflects and transferred heat from endothermic evaporation / adsorption and exothermic condensation / adsorption processes.
- A heat source arising from microbial processes, which is proportional to the oxygen consumption during aerobic respiration.

Dienes [7] studied the thermal decomposition in a slab and found that time-independent solutions for the spatial structure of temperature, considering a slab with isothermal boundaries subjected to exothermic reaction and uniform plastic heating. It is well known that thermal decomposition of different materials is dependent on size, shape and surface or environmental temperature as well as the physical properties of the material and environment. In other words for any given geometry, there is a critical size and surface temperature above which the heat generation inside the solid exceeds the heat dissipation to the surroundings [8]. Many commonly used materials have obvious reactivity hazards. For example explosives, laboratory chemicals, and raw materials are used to make plastics and other useful products. They are handled safely because their hazards have been recognized and controlled so that undesirable events do not happen. Testing for reactive materials include testing for water reactivity, shock sensitivity, dust explosiveness and thermal stability in actual storage and handling configurations. Reactive materials are commonly regarded as those materials that can be hazardous by themselves when caused to react by heat, pressure, shock, friction, catalyst or by contact with air or water [9]. [10] studied the thermal explosion of autocatalytic reaction. The thermal explosion in the presence of heat generation by an autocatalytic reaction was first discussed analytically by [11], and [12]. They defined criticality as a point at which two lobes of the loci of maximal touched using the Frank-Kamenetskii exponential approximation for the Arrhenius rate term. The effect of reactant consumption was considered in most cases solely in terms of a reaction rate decreasing uniformly with time, the effect on pre-explosion self heating being negligible when the heat of the reaction is sufficiently large.

There are specific criteria, which determine spontaneous change in behaviour of thermal ignition. Thermal ignition is a type of instability in which the combustible at a negligible rate is brought to a condition in which it is reacting at an appreciable rate.

While in thermal ignition no momentum is created by the chemical reactions, in a reactive viscous flow it may be very significant to include the momentum equation of the reactive system to accommodate the flow dynamics. The assumption of constant density approximation is well-founded assumption because it can be used to separate the momentum equation from the energy equation [13]. The problem of thermal explosion has been widely explained in the literature. Many researchers developed the basic theory of the phenomenon of thermal explosion. Since then more complicated models have been suggested. The problem of exothermic chemically reactive material in a slab obeys the Arrhenius law and accounts for temperature dependence of a pre-exponential factor based on the assumptions that the reacting material is motionless, the heat losses are caused by the thermal conductivity of the reacting material and the chemical reaction proceeds non-uniformly over the vessel volume [14]. Meanwhile, the explosive and non-explosive properties of chemical reactions are the main mathematical challenge of the thermal explosion theory [15]. The steady-state solutions for the strongly exothermic decomposition of a combustible material uniformly distributed in heated symmetrical geometries under Arrhenius kinetics, neglecting the consumption of the material, are investigated. Analytical solutions are constructed for the governing nonlinear boundary value problem using perturbation technique together with a special type of Hermite-Pade approximants and important properties of the temperature field including bifurcations and thermal criticality are explained, for observed that at very large activation energy, thermal explosions criticality varies from one symmetric geometry to another, [16]. [17] derived a mathematical model to predict the heating up of large scale wood piles has been developed. This model includes the heat production from chemical physical and microbial exothermal processes. The storage of wood chips in large open air piles with thousands of tons of material is susceptible to the self ignition of the bulk material.

1.1. Definition of terms

Arrhenius reaction

When the temperature increases, the rate of a chemical reaction increases also. Iron rusts, food spoils, or bread rises more rapidly when the conditions are warm than when they are cool. These qualitative observations which we all make were expressed in quantitative form only with measurements of reaction rates near the end of the

nineteenth century. At this time what we now call the Arrhenius rate law was established, primarily by the Swedish chemist Avante Arrhenius: *the rate of a chemical reaction increases exponentially with the absolute temperature*. In short, the Arrhenius equation relates "the rate constant k of chemical reactions to the temperature T (in absolute temperature in Kelvin or Rankine) and activation energy E_a ", as shown below:

$$k = Ae^{-E_a/RT}$$

where A is the pre-exponential factor or simply the prefactor and R is the gas constant. The units of the pre-exponential factor are identical to those of the rate constant and will vary depending on the order of the reaction. If the reaction is first order it has the units s^{-1} , and for that reason it is often called the frequency factor or attempt frequency of the reaction. Most simply, k is the number of collisions which result in a reaction per second, A is the total number of collisions (leading to a reaction or not) per second and $e^{-E_a/RT}$ is the probability that any given collision will result in a reaction. When the activation energy is given in molecular units instead of molar units, e.g. joules per molecule instead of joules per mole, the Boltzmann constant is used instead of the gas constant. It can be seen that either increasing the temperature or decreasing the activation energy (for example through the use of catalysts) will result in an increase in rate of reaction.

Bimolecular reaction

Bimolecular reaction is a chemical reaction involving the collision and combination of two reactants to form an activated complex in an elementary reaction (a reaction that cannot be broken down into smaller steps).

Exothermic reaction

Exothermic reaction is a chemical reaction that is accompanied by the release of heat. In other words, the energy needed for the reaction to occur is less than the total energy released. As a result of this, the extra energy is released, usually in the form of heat. This can be expressed in form of a chemical equation as:

reactants \rightarrow products + energy

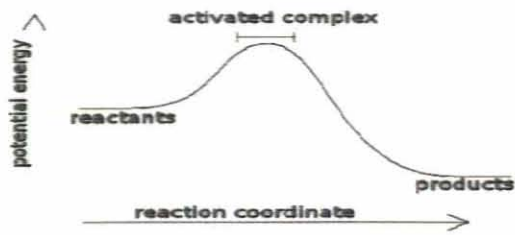


Figure 1.01: A sketch of an exothermic reaction



Figure 1.02: Picture showing the explosions of materials under strong exothermic reactions [36].

Ignition temperature

Ignition temperature is the temperature to which a combustible material must be raised before it begins to burn.

Reactive interactions

Reactive interactions require the combining of two or more materials to pose a hazardous situation by chemical reaction.

Reactive materials

Reactive materials are commonly regarded as those materials that can be hazardous by themselves when caused to react by heat, pressure, shock, friction, catalyst or by contact with air or water.

Reactivity

Reactivity is the tendency of a combination of materials to undergo chemical change under the right conditions.

Thermal ignition

Thermal ignition is a type of instability in which the heat produced by reacting combustible materials exceeds the heat loss, hence, leading to large accumulation of heat in the system and thermal runaway.

Heat

Heat from the sun is the driving force of life on Earth. The science of heat and its relation to work is thermodynamics. Heat flow can be created in many ways. In physics and thermodynamics, heat is the process of energy transfer from one body or system due to thermal contact, which in turn is defined as an energy transfer to a body in any other way than due to work performed on the body. When an infinitesimal amount of heat δQ is transferred to a body in thermal equilibrium at absolute temperature T in a reversible way, then it is given by the quantity TdS , [18] where S is the entropy of the body. A related term is thermal energy, loosely defined as the energy of a body that increases with its temperature. Heat is also loosely referred to as thermal energy, although many definitions require this thermal energy to actually be in the process of movement between one body and another to be technically called heat (otherwise, many sources prefer to continue to refer to the static quantity as "thermal energy"). Heat is also known as "Energy". Energy transfer by heat can occur between objects by radiation, conduction and convection. Temperature is used as a measure of the internal energy or enthalpy, that is the level of elementary motion giving rise to heat transfer. Energy can only be transferred by heat between objects - or areas within an object - with different temperatures (as given by the zeroth law of thermodynamics). This transfer happens spontaneously only in the direction of the colder body (as per the second law of thermodynamics). The transfer of energy by heat from one object to another object with an equal or higher temperature can happen only with the aid of a heat pump, which does work. The first law of thermodynamics states that the energy of a closed system is conserved. Therefore, to change the energy of a system, energy must be transferred to or from the system. Heat and work are the only two mechanisms by which energy can be transferred to or from a control mass. Heat is the energy transferred to the body in any other way. This definition of heat applies generally, it does not appeal to any notion of thermal equilibrium. In case of bodies close to thermal equilibrium where notions such as the temperature can be defined, heat transfer can be related to temperature difference between bodies. It is an

irreversible process that leads to the bodies coming closer to mutual thermal equilibrium. The unit for the amount of energy transferred by heat in the International System of Units SI is the joule (J). The unit for the rate of heat transfer is the watt ($W = J/s$). Specific heat is defined as the amount of energy that has to be transferred to or from one unit of mass or mole of a substance to change its temperature by one degree. Specific heat is a property, which means that it depends on the substance under consideration and its state as specified by its properties. Fuels, when burned, release much of the energy in the chemical bonds of their molecules. Upon changing from one phase to another, a pure substance releases or absorbs heat without its temperature changing. The amount of heat transfer during a phase change is known as latent heat and depends primarily on the substance and its state. The total amount of energy transferred through heat transfer is conventionally abbreviated as Q . The conventional sign convention is that when a body releases heat into its surroundings, $Q < 0$ (-); when a body absorbs heat from its surroundings, $Q > 0$ (+). It is measured in watts. Heat flux is defined as rate of heat transfer per unit cross-sectional area, and is denoted q , resulting in units of watts per square meter, though slightly different notation conventions can be used.

Heat transfer mechanisms

Heat tends to move from a high-temperature region to a low-temperature region. This heat transfer may occur by the mechanisms of conduction and radiation. In engineering, the term convective heat transfer is used to describe the combined effects of conduction and fluid flow and is regarded as a third mechanism of heat transfer.

Conduction

Conduction is the most significant means of heat transfer in a solid. On a microscopic scale, conduction occurs as hot, rapidly moving or vibrating atoms and molecules interact with neighboring atoms and molecules, transferring some of their energy (heat) to these neighboring atoms, [19]. In insulators the heat flux is carried almost entirely by phonon vibrations. Fire used to test the heat transfer through firestops and penetrants used in construction listing and approval use and compliance. The "electron fluid" of a conductive metallic solid conducts nearly all of the heat flux through the solid. Phonon flux is still present, but carries less than 1% of the energy. Electrons also conduct electric current through conductive solids, and the thermal and

electrical conductivities of most metals have about the same ratio. A good electrical conductor, such as copper, usually also conducts heat well. The Peltier-Seebeck effect exhibits the propensity of electrons to conduct heat through an electrically conductive solid. Thermoelectricity is caused by the relationship between electrons, heat fluxes and electrical currents.

Convection

Convection is usually the dominant form of heat transfer in liquids and gases. This is a term used to characterize the combined effects of conduction and fluid flow. In convection, enthalpy transfer occurs by the movement of hot or cold portions of the fluid together with heat transfer by conduction. Commonly an increase in temperature produces a reduction in density. Hence, when water is heated on a stove, hot water from the bottom of the pan rises, displacing the colder denser liquid which falls. Mixing and conduction result eventually in a nearly homogeneous density and even temperature. Two types of convection are commonly distinguished, free convection, in which gravity and buoyancy forces drive the fluid movement, and forced convection, where a fan, stirrer, or other means is used to move the fluid. Buoyant convection is due to the effects of gravity, and hence does not occur in microgravity environments.

Radiation

Radiation is the only form of heat transfer that can occur in the absence of any form of medium (i.e., through a vacuum). Thermal radiation is a direct result of the movements of atoms and molecules in a material. Since these atoms and molecules are composed of charged particles (protons and electrons), their movements result in the emission of electromagnetic radiation, which carries energy away from the surface. At the same time, the surface is constantly bombarded by radiation from the surroundings, resulting in the transfer of energy to the surface. Since the amount of emitted radiation increases with increasing temperature, a net transfer of energy from higher temperatures to lower temperatures results.

1.2. STATEMENT OF THE PROBLEM

There are serious challenges of dangerous reactive materials which justify the analysis of thermal decomposition of reactive material in a slab. Because many facilities and systems have chemically reactive materials that may have serious consequences if

they are not handled, used and stored properly. Previous studies of the thermal decomposition of reactive material dealt with different dimensional shapes like cylindrical, rectangular parallelepiped, sphere, etc. In this study we consider the special case of thermal decomposition of reactive material in a slab. The problem here is to cover this gap by analysing the thermal decomposition of a reactive material in a slab and investigate ways of minimizing the dangers of thermal decomposition.

1.3. OBJECTIVES OF THE STUDY

The general objective is to analyze a mathematical model of thermal decomposition for reactive material in a slab.

Specific objectives of this study are therefore:

- (i) To derive a mathematical model for heat transfer and thermal stability in a slab subjected to Arrhenius kinetics
- (ii) To investigate the transient effect on thermal decomposition in a slab under exothermic reaction for moderate activation energy.
- (iii) To determine the possibility of bifurcation or blowup when the reaction parameter Frank-Kamenetskii exceeds certain threshold values.
- (iv) To investigate the effects of variable heat loss on the thermal decomposition of reactive material in a slab.

1.4. SIGNIFICANCE OF THE STUDY

The output of this study will be of engineering and industrial interest in understanding how to combat the dangers of thermal decomposition of reactive material that may occur during handling, usage and storage of materials capable of spontaneous exothermic reactions. For instance, self heating of agricultural materials commonly stored in silos like Icing sugar, Maize, Wheat, Barley, Alfalfa, Bread making wheat and Soybean; the heating-up of large-scale wood piles; efficient operation of autocatalytic ignition in automobile, etc. Computations in larger geometries have shown that the global model can predict the achievement of critical conditions and therefore help to identify possible self-ignition scenarios and avoid undesired fires.

1.5. RESEARCH HYPOTHESES

- (i) At a fixed reaction rate, the material temperature increases with time until a steady state temperature is attained.

- (ii) The model of thermal decomposition of reactive material in a slab exhibits the phenomenon of bifurcation or blowup when the reaction parameter Frank-Kamenetskii exceeds certain threshold values.
- (iii) Thermal decomposition is affected by boundary conditions and other parameters.

1.6. METHODOLOGY

This study will formulate and analyze models for heat transfer and thermal stability in a slab under Arrhenius kinetic. The nonlinear conservation of energy and mass equations under the one-dimensional assumption will be derived. In order to reduce the number of parameters in the model, the dimensionless and rescaling variables will be introduced. Both analytical and numerical methods (semi-discretization finite difference techniques) will be applied to tackle the model problems. The results will be presented graphically to explain the thermal decomposition of reactive material in a slab for different values of the parameters in the model. The computer packages that will be used for the model simulation are Maple and Matlab software.

DERIVATION OF BASIC EQUATIONS FOR THE PROBLEM

The problem under investigation involves two important variables i.e. the slab temperature and the oxygen concentration. In this chapter, we derive the basic differential equations for the problem.

2.1 ENERGY EQUATION

In order to derive the energy equation we need to consider the zeroth and the first law of thermodynamics

2.1.1 The Zeroth Law of Thermodynamics

There exists the temperature T such that when two systems that are in contact are in thermal equilibrium, then T is the same in both systems. T is called the absolute temperature [20].

2.1.2 The First Law of Thermodynamics

This law expresses principle of conservation of energy which states that there exists a variable of state E such that if a system is transformed from one state of equilibrium to another by the process in which the amount of work W is done on the system by its surroundings and an amount of heat Q is added to the system from the surrounding, then the difference between the initial and final values of the system E_i and E_f is given by

$$E_f - E_i = Q + W, \quad (2.1.2.1)$$

In differential form, we have

$$dE = dQ + dW \quad (2.1.2.2)$$

or

$$\frac{dE}{dt} = \frac{dQ}{dt} + \frac{dW}{dt}. \quad (2.1.2.3)$$

In order to determine the work, we consider the contribution from component σ_y of stress.

The work in unit time is given by

$$\frac{\partial(W\sigma_{xx})}{\partial t} = dydz \left[-U\sigma_{xx} + \left(U + \frac{\partial U}{\partial x} dx \right) \left(\sigma_{xx} + \frac{\partial \sigma_{xx}}{\partial x} dx \right) \right] = \Delta V \frac{\partial(U\sigma_{xx})}{\partial x}, \quad (2.1.2.4)$$

where, $\Delta V = dxdydz$. The total work done by the stress per unit mass on deforming elements of fluid ΔV is given by

$$\frac{1}{\rho} \frac{\partial(\sigma_{ij}U_j)}{\partial x_i} = \frac{1}{2} \left(\frac{\partial \sigma_{ij}}{\partial x_i} + \sigma_{ij} \frac{\partial U_j}{\partial x_i} \right), \quad (2.1.2.5)$$

where σ_{ij} is the stress acting in the x_i on the force whose normal lies in the x_j direction.

For the equation of fluid motion, we have

$$\rho \frac{\partial U_i}{\partial t} = \frac{\partial \sigma_{ij}}{\partial x_j} \quad (2.1.2.6)$$

and

$$U_j \frac{\partial \sigma_{ij}}{\partial x_i} = \rho \frac{\partial U_i}{\partial t} U_j = \frac{\rho}{2} \frac{d(U_i U_j)}{dt} \quad (2.1.2.7)$$

which is clearly the change in kinematic energy of fluid element following motion. The remaining term in (2.5.3.2.6) represents the rate of depression of energy per unit mass.

Substituting $\sigma_{ij} = -p\delta_{ij} + \mu e_{ij}$ we get

$$\frac{\partial W}{\partial t} = \frac{1}{2} \frac{\partial(U_i U_j)}{\partial t} - \frac{p}{\rho} \sigma_{ij} \frac{\partial U_j}{\partial x_i} + \nu \frac{\partial U_i}{\partial x_i} \left(\frac{\partial U_i}{\partial x_i} + \frac{\partial U_j}{\partial x_j} \right) \quad (2.1.2.8)$$

$$\text{but } \sigma_{ij} \frac{\partial U_j}{\partial x_i} = \frac{\partial U_i}{\partial x_i} = 0$$

It is clear that only viscous forces and not pressure forces contribute to energy dissipation, now define the energy dissipation function Φ by

$$\Phi = \frac{\partial U_i}{\partial x_i} \left(\frac{\partial U_i}{\partial x_i} + \frac{\partial U_j}{\partial x_j} \right) = \frac{1}{2} \left(\frac{\partial U_i}{\partial x_i} + \frac{\partial U_j}{\partial x_j} \right)^2 \quad (2.1.2.9)$$

which shows that $\Phi \geq 0$ and we have,

$$\frac{dW}{dt} = \frac{1}{2} \frac{d}{dt} (U_i U_j) + \nu \Phi \quad (2.1.2.10)$$

Similarly the heat transferred to the system from the surrounding is Q . We shall neglect the transfer of heat by radiation and consider only that by conduction. If we consider the element of the volume, $dv = dxdydz$ of the mass ρdv , then the change in

the total energy dE is equal to the change in the internal energy ρdve and a change in kinetic energy of an amount

$$d\left[\frac{1}{2}\rho dv(U_1^2 + U_2^2 + U_3^2)\right] \quad (2.1.2.11)$$

Neglecting change in the potential energy, we then have

$$\frac{dE}{dt} = \rho dv \left[\frac{de}{dt} + \frac{1}{2} \frac{d(U_1^2 + U_2^2 + U_3^2)}{dt} \right], \quad (2.1.2.12)$$

where e is the thermal energy per unit mass.

2.1.3 Fourier Heat Conduction

This law states that the heat flux q per unit area is proportional to the temperature gradient, i.e.,

$$q = \frac{1}{A} \frac{\partial Q}{\partial t} = -k \frac{\partial T}{\partial n} \quad (2.1.3.1)$$

or, $\mathbf{q} = -k\nabla T$, where k is the thermal conductivity.

The negative signifies that the heat flux is reckoned as positive in the direction of temperature gradient (i.e. heat flux in the direction of decreasing temperature). Hence the amount of heat transferred into volume dv through surface elements which are normal to x direction is equal to

$$\left(-k \frac{\partial T}{\partial x}\right) dydz, \quad (2.1.3.2)$$

The amount of heat leaving the volume is given by

$$\left[k \frac{\partial T}{\partial x} + \frac{\partial}{\partial x} \left(k \frac{\partial T}{\partial x}\right) dx\right] dydz, \quad (2.1.3.3)$$

thus the amount of heat added by conduction in the x direction during time dt to volume dv is

$$dt \cdot dv \left(k \frac{\partial T}{\partial x}\right).$$

Hence, the total amount of heat added in all direction is given by

$$\frac{\partial Q}{\partial t} = dv \left[\frac{\partial}{\partial x} \left(k \frac{\partial T}{\partial x}\right) + \frac{\partial}{\partial y} \left(k \frac{\partial T}{\partial y}\right) + \frac{\partial}{\partial z} \left(k \frac{\partial T}{\partial z}\right) \right] \quad (2.1.3.4)$$

Using equation (2.1.3.3) and (2.1.3.4) we obtain

$$\rho \frac{\partial e}{\partial t} = \frac{\partial}{\partial x} \left(k \frac{\partial T}{\partial x} \right) + \frac{\partial}{\partial y} \left(k \frac{\partial T}{\partial y} \right) + \frac{\partial}{\partial z} \left(k \frac{\partial T}{\partial z} \right) + \nu \Phi \quad (2.1.3.5)$$

where,

$$\Phi = 2 \left\{ \left(\frac{\partial U_1}{\partial x} \right)^2 + \left(\frac{\partial U_2}{\partial y} \right)^2 + \left(\frac{\partial U_3}{\partial z} \right)^2 \right\} + \left(\frac{\partial U_1}{\partial y} + \frac{\partial U_2}{\partial x} \right)^2 + \left(\frac{\partial U_3}{\partial y} + \frac{\partial U_2}{\partial z} \right)^2 + \left(\frac{\partial U_1}{\partial z} + \frac{\partial U_3}{\partial x} \right)^2.$$

Equation (2.1.3.5) holds for an incompressible fluid. For perfect fluid,

$$\frac{de}{dt} = C_v \frac{dT}{dt}, (de = C_v dT), \quad (2.1.3.6)$$

equation (2.1.3.5) now takes the form

$$\rho C_v \frac{dT}{dt} = \nabla \cdot (k \nabla T) + \mu \Phi + H(T) \quad (2.1.3.7)$$

where C_v is the specific heat at constant volume and $H(T)$ is the heat source/sink term added to the equation depending whether it is positive or negative. From differential calculus, the left hand side of equation (2.1.3.7) can be written as

$$\rho C_v \frac{dT}{dt} = \rho C_v \left(\frac{\partial T}{\partial t} + (V \cdot \nabla) T \right), \quad (2.1.3.8)$$

where V is the velocity vector. Incorporating equation (2.1.3.8) into (2.1.3.7), we obtain the energy balance equation as

$$\rho C_v \left(\frac{\partial T}{\partial t} + (V \cdot \nabla) T \right) = \nabla \cdot (k \nabla T) + \mu \Phi + H(T) \quad (2.1.3.9)$$

In this present study, $V = 0$ and $\Phi = 0$ since the fluid flow is not present, however, we are interested in the thermal decomposition in a slab due to internal heat generation (i.e. $H(T)$ is positive) as a result of an exothermic n^{th} order oxidation chemical reaction in which the consumption of oxygen (reactant concentration) is taken into account and the thermal conductivity (k) is assumed to be constant. Equation (2.1.3.9) then becomes

$$\rho C_v \frac{\partial T}{\partial t} = k \nabla^2 T + H(T, C) \quad (2.1.3.10)$$

In the following chapters appropriate forms of the heat source term $H(T, C)$ due to exothermic chemical kinetics will be utilised in the investigation.

2.2 CONCENTRATION EQUATION

Mass transfer is another important concept in the field of chemical engineering and science in general. Mass transfer is the process responsible for the conversion of one component species to another. In many systems, mass transfer process is made up of advection, diffusion, and chemical kinetics. Advective transport is a function of the average linear velocity due to fluid flow. Diffusion is the macroscopic result of random thermal motion on a microscopic scale. For example, in the diagram below, oxygen and nitrogen molecules move in random directions. If there are more oxygen molecules on the left side of the plane A-A than on the right, more molecules will cross to the right than to the left: there will be a net flux even though the motion of each individual molecule is completely random.

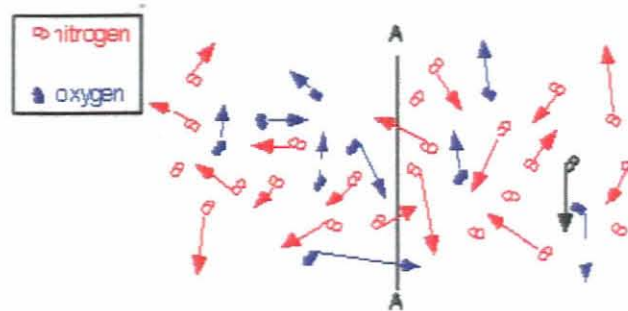


Figure 2.2.01: Change in Mass flux in a given volume

Following the Fick's Law, the flux is proportional to the gradient in concentration (C) and is given by

$$J = -D\nabla C, \quad (2.2.01)$$

where

- J – The Mass Flux – Flux is the movement of objects from one point to another in a given time. The flux is what we are measuring when studying diffusion.
- D – Mass Diffusivity – The diffusivity is the constant that describes how fast or slow an object diffuses.

The chemical kinetics can be the sum of sorption, desorption, decay, abiotic reaction, and metabolism by bacteria. It may also be a function of multiple solutes. Moreover, the rate of chemical reaction typically kinetically limit mass transfer processes.

Consider a given volume in which mass transfer process takes place (see Figure 2.2.01 below). The change in the number of molecules with time is the difference between the flux going in and the flux going out.

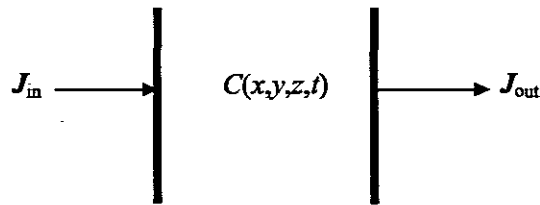


Figure 2.2.02: Change in Mass flux in a given volume

Using equation (2.2.01), the time rate of accumulation of chemical species in the volume is given as

$$\frac{dC}{dt} = \nabla \cdot (D\nabla C) + R(C), \quad (2.2.02)$$

where $R(C)$ term in equation (2.2.02) represents the conversion of one component species to another by chemical kinetics. When $R(C)$ is negative, the reactant species is been consumed through the process. From differential calculus, the left hand side of equation (2.2.02) can be written as

$$\frac{dC}{dt} = \frac{\partial C}{\partial t} + (V \cdot \nabla)C, \quad (2.2.03)$$

where V is the velocity vector. Incorporating equation (2.2.03) into (2.2.02), we obtain the fundamental equation for advective-dispersive-reactive transport of chemicals and microbes [21] as:

$$\frac{\partial C}{\partial t} + (V \cdot \nabla)C = \nabla \cdot (D\nabla C) + R(C). \quad (2.2.04)$$

In this present study, $V = 0$ since the fluid flow is not present, hence the advective term does not contribute to mass transport of chemical species, however, we are interested in the thermal decomposition in a slab due to an n^{th} order oxidation chemical reaction in which the consumption of oxygen (a reactant) is taken into account (i.e. the term $R(C)$ is negative) and the mass diffusivity (D) is assumed to be constant. Equation (2.2.04) then becomes

$$\frac{\partial C}{\partial t} = D\nabla^2 C - R(C, T). \quad (2.2.05)$$

In the following chapters appropriate forms of the chemical kinetics $R(C, T)$ will be utilised in the investigation.

3.1. Transient heating of slab under an n^{th} order oxidation chemical reaction

3.1.1. Summary

In this chapter we explore the applicability of one-step irreversible chemical kinetics with reactant consumption and n^{th} order oxidation exothermic reaction to transient heating of combustible materials in the presence of convective heat transfer to the ambient. It is assumed that the material surface exchanges oxygen with its surroundings. The governing nonlinear partial differential equations are solved numerically by method of lines (MOL), with finite difference schemes used for the discretisation of the spatial derivatives. Graphical results are presented and discussed quantitatively with respect to various embedded parameters controlling the systems. The crucial role played by the boundary conditions in determining the location of the maximum heating are demonstrated.

3.1.2. Introduction

Transient heating of combustible materials due to oxidation chemical reaction plays a significant role in many industrial applications [22]. These processes include but are not limited to: heavy oil recovery, storage of cellulosic materials, the pyrolysis of biomass and coal, the combustion of solids, waste incineration, coal gasification, etc. Moreover, the knowledge of the mathematical model of these complex chemical systems is essential for the accurate and reliable design of the systems [23]. It has a significant impact on the equipment needed in chemical production plants and storage of industrial waste fuel. The problem of an accurate design of chemical reactors and storage facilities is not only economical; it is directly related to safety issues and hazard assessment. Simplified or inaccurate design of these industrial equipments can lead to disastrous consequences [24]. Without adequate knowledge of the system, exothermic chemical process can accelerate significantly leading to runaway reaction, possible explosion, economical losses and cause emission of carbon dioxide and of toxic gases, like carbon monoxide through incomplete combustion. For example, this

was determined to be the cause of the explosion on 8 April 1998 at Morton Chemical International (now Rohm & Haas) in Paterson, NJ, USA [25]. This reactor explosion had serious consequences, injuring nine people and two seriously. Hazardous materials were also released into the environment causing significant damage.

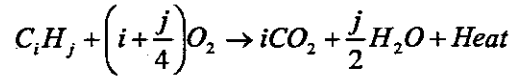
An extensive review of detailed chemical kinetic models for the heating-up of combustible materials has been written by Simmie [26], his review considered post-1994 work and was focused on the modelling of hydrocarbon fuels oxidation in the gas phase by detailed chemical kinetics and those experiments which validate them. Further, thermal explosion analysis has received much attention in the literature [14], [27,28]. Several studies have been directed towards obtaining critical conditions for thermal ignition to occur, in the form of a critical value for the Frank-Kamenetskii parameter [29]. Usually, chemical process includes many, up to a several hundred, intermediate elementary reactions [30]. For example, in combustion science, it is very common to use complex multi-step reaction mechanisms to predict the oxidation of hydrocarbons [31]. However, the use of one-step decomposition kinetics clearly simplifies the complicated chemistry involved in the problem but is both practical and necessary without additional information about the individual decomposition reaction steps [32,33]. Meanwhile, analytical solutions of the partial differential equations governing transient heating of the combustible material undergoing oxidation reactions are usually impossible or extremely difficult to obtain. The exothermic nature of such reactions leads to complex nonlinear transient interaction of heat conduction, mass diffusion, and chemical reactions, resulting in steep concentration and temperature gradients [34]. In such circumstances, a better understanding of the system behaviour can only be accomplished by conducting numerical simulations to capture the frontal behaviour of the process [35].

As far as is known to the author, investigation of transient heating of combustible materials undergoing higher-order oxidation chemical reaction with convective heat and oxygen exchange at the material surface have never been reported in the literature. Hence, the objective of this study is therefore to perform a numerical study of transient heating of combustible materials with Arrhenius type of one-step n th order oxidation reaction kinetics in the presence of convective heat and oxygen exchange with the ambient. This paper is organized as follows. Firstly, the governing partial differential equations for oxidation reactions are presented and solved numerically using the semi-discretization finite difference technique known as

method of lines. Pertinent results are presented graphically and discussed quantitatively.

3.1.3. Mathematical model

The geometry of the problem is depicted in Fig. 3.1.3.1. It is assumed that the combustible material is undergoing an n th order oxidation chemical reaction. The complicated chemistry involved in the problem is simplified by assuming a one-step finite-rate irreversible reaction between the combustible material (hydrocarbon) and the oxygen of the air i.e.,



[Combustible material + Oxygen \rightarrow Heat + Carbondioxide + Water]

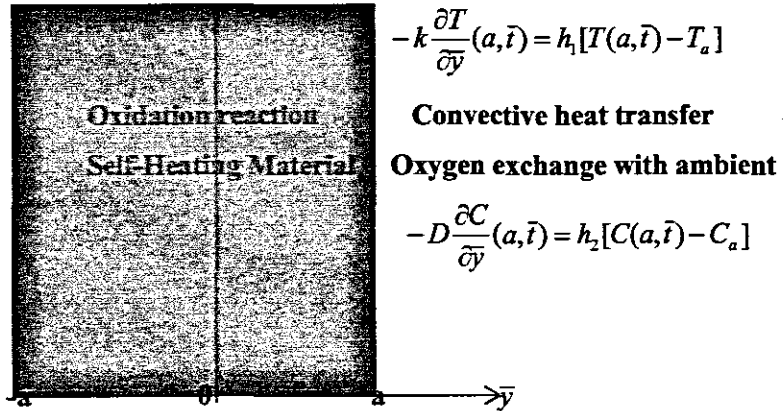


Figure 3.1.3.1: Geometry of the Problem

Following [6, 13, 14], the nonlinear partial differential equations describing the temperature and oxygen concentration in the combustible material can be written as;

$$\rho c_p \frac{\partial T}{\partial \bar{t}} = k \frac{\partial^2 T}{\partial \bar{y}^2} + Q A \left(\frac{KT}{\bar{u}} \right)^m (C - C_0)^n e^{-\frac{E}{RT}}, \quad (3.1.3.1)$$

$$\frac{\partial C}{\partial \bar{t}} = D \frac{\partial^2 C}{\partial \bar{y}^2} - A \left(\frac{KT}{\bar{u}} \right)^m (C - C_0)^n e^{-\frac{E}{RT}}, \quad (3.1.3.2)$$

with initial and boundary conditions as

$$T(\bar{y},0) = T_0, \quad C(\bar{y},0) = C_0 \quad (3.1.3.3)$$

$$-k \frac{\partial T}{\partial \bar{y}}(a, \bar{t}) = h_1 [T(a, \bar{t}) - T_a], \quad -D \frac{\partial C}{\partial \bar{y}}(a, \bar{t}) = h_2 [C(a, \bar{t}) - C_a], \quad (3.1.3.4)$$

$$\frac{\partial T}{\partial \bar{y}}(0, \bar{t}) = \frac{\partial C}{\partial \bar{y}}(0, \bar{t}) = 0, \quad (3.1.3.5)$$

where T is the absolute temperature, T_a is the ambient temperature, \bar{t} is the time, C_a is the oxygen concentration in the surrounding air, C_0 is the initial concentration of oxygen in the material, ρ is the density, c_p specific heat at constant pressure, T_0 is the slab initial temperature, k is the thermal conductivity of the material, Q is the exothermicity, A is the rate constant, E is the activation energy, R is the universal gas constant, l is the Planck's number, K is the Boltzmann's constant, ν is the vibration frequency, a is the slab half width, \bar{y} is the distance measured transverse direction, h_1 is the heat transfer between the material and its surroundings, D is the diffusivity of oxygen in the material, h_2 is the transfer of oxygen from the material to its surroundings, n is the chemical reaction order and m is the numerical exponent such that $m = \{-2, 0, \frac{1}{2}\}$ represent numerical exponent for Sensitised, Arrhenius and Bimolecular kinetics respectively (see [1, 6]). We introduce the following dimensionless variables into Eqs. (3.1.3.1)- (3.1.3.5)

$$Bi = \frac{h_1 a}{k}, \gamma = \frac{h_2 a}{D}, \phi = \frac{(C - C_0)}{(C_a - C_0)}, \theta = \frac{E(T - T_0)}{RT_0^2}, \theta_a = \frac{E(T_a - T_0)}{RT_0^2}, y = \frac{\bar{y}}{a}, t = \frac{k \bar{t}}{\rho c_p a^2}, \quad (3.1.3.6)$$

$$\varepsilon = \frac{RT_0}{E}, \alpha = \frac{k}{D \rho c_p}, \lambda = \frac{QAEa(C_a - C_0)^n}{kRT_0^2} \left[\frac{KT_0}{l} \right]^m e^{\frac{E}{RT_0}}, \beta = \frac{kRT_0^2}{DQRC_a - C_0},$$

and we obtain the dimensionless governing equations as

$$\frac{\partial \theta}{\partial t} = \frac{\partial^2 \theta}{\partial y^2} + \lambda(1 + \varepsilon \theta)^m \phi^n e^{\frac{\theta}{1 + \varepsilon \theta}}, \quad (3.1.3.7)$$

$$\alpha \frac{\partial \phi}{\partial t} = \frac{\partial^2 \phi}{\partial y^2} - \lambda \beta (1 + \varepsilon \theta)^m \phi^n e^{\frac{\theta}{1 + \varepsilon \theta}}, \quad (3.1.3.8)$$

and the associated boundary conditions (3.1.3.3)-(3.1.3.5) become

$$\theta(y,0) = 0, \quad \phi(y,0) = 0 \quad (3.1.3.9)$$

$$\frac{\partial \theta}{\partial y}(1,t) = -Bi[\theta(1,t) - \theta_a], \quad \frac{\partial \phi}{\partial y}(1,t) = -\gamma[\phi(1,t) - 1] \quad (3.1.3.10)$$

$$\frac{\partial \theta}{\partial y}(0, t) = \frac{\partial \phi}{\partial y}(0, t) = 0, \quad (3.1.3.11)$$

where $\lambda, \varepsilon, \beta, \alpha, \gamma, Bi$ represent the Frank-Kamenetskii parameter, activation energy parameter, Oxygen consumption rate parameter, material surface oxygen transfer parameter and the Biot number respectively. A body of material releasing heat to its surroundings may achieve a safe steady-state where the temperature of the body reaches some moderate value and stabilizes. However, when the rate of heat generation of the material exceeds the rate of heat loss to the surroundings, then ignition can occur. In the following section, Equations. (3.1.3.7)-(3.1.3.11) are solved numerically using method of lines.

3.1.4. Numerical Procedure

For nonlinear parabolic problems such as Eqs.(3.1.3.7)-(3.1.3.11), the method of lines is a powerful solution technique, where the spatial derivatives are discretised transforming the governing partial differential equations (PDEs) into a system of ordinary differential equations (ODEs) [15]. Usually the chemistry involved in the combustion process introduces stiffness and / or multiple time scales so the availability of robust stiff ODE integrators gives an advantage to this method. We have adopted the method of lines as our solution technique.

The governing equations (3.1.3.7)-(3.1.3.8) with the initial and boundary conditions (3.1.3.9)-(3.1.3.11) are transformed into a system of ODEs using finite differences for the spatial derivatives. The discretization is based on a linear Cartesian mesh and uniform grid. Firstly, a partition of the spatial interval $0 \leq y \leq 1$ is introduced. We divide it into N equal parts and define grid size $\Delta y = 1/N$ and grid points $y_i = (i-1)\Delta y, 1 \leq i \leq N+1$. The first and the second spatial derivatives in Eqs.(3.1.3.7)-(3.1.3.11) are approximated with second-order central differences. Let $\theta_i(t)$ and $\phi_i(t)$ be approximations of $\theta(y_i, t)$ and $\phi(y_i, t)$ respectively, then the semi-discrete system for the problem reads:

$$\frac{d\theta_i}{dt} = \frac{1}{(\Delta y)^2} (\theta_{i+1} - 2\theta_i + \theta_{i-1}) + \lambda(1 + \varepsilon\theta_i)^m \phi_i^n \left[e^{\left(\frac{\theta_i}{1 + \varepsilon\theta_i} \right)} \right], \quad (3.1.4.1)$$

$$\alpha \frac{d\phi_i}{dt} = \frac{1}{(\Delta y)^2} (\phi_{i+1} - 2\phi_i + \phi_{i-1}) - \lambda f(1 + \varepsilon\theta_i)^m \phi_i^n \left[e^{\left(\frac{\theta_i}{1 + \varepsilon\theta_i} \right)} \right], \quad (3.1.4.2)$$

with initial conditions

$$\theta_i(0) = 0 \quad \phi_i(0) = 0, \quad 1 \leq i \leq N+1. \quad (3.1.4.3)$$

The equations corresponding to the first and last grid points are modified to incorporate the boundary conditions, i.e.

$$\left. \frac{\partial \theta}{\partial y} \right|_{y=0} = \frac{\theta_3 - \theta_1}{2\Delta y} = 0, \quad \theta_{N+1} = \frac{\theta_{N-1} + 2\Delta y Bi \theta_a}{1 + 2\Delta y Bi}, \quad (3.1.4.4)$$

$$\left. \frac{\partial \phi}{\partial y} \right|_{y=0} = \frac{\phi_3 - \phi_1}{2\Delta y} = 0, \quad \phi_{N+1} = \frac{\phi_{N-1} + 2\gamma \Delta y}{1 + 2\gamma \Delta y}. \quad (3.1.4.5)$$

In Equations. (3.1.4.1)-(3.1.4.2), there is only one independent variable, so they are ordinary differential equations. Since they are first order, and the initial conditions for all variables are known, the problem is an initial value problem. The MAPLE program is employed to integrate the sets of differential equations using a fourth order Runge-Kutta method.

3.1.5. Results and Discussion

In order to get a clear insight into the thermal development in the system due to a one-step exothermic oxidation chemical reaction, we have assigned numerical values to the parameters encountered in the problem. At initial stage, the temperature of the slab is assumed to be slightly below that of the ambient and there is possibility of convective heat exchange with the ambient. Similarly, the oxygen concentration in the slab is below that of the ambient and the material exchange oxygen with the ambient at its surface.

A. Effect of various parameters on temperature profiles

Figs. (3.1.5.2)-(3.1.5.9) illustrate the effects of various thermophysical parameters on the slab temperature profiles. The time evolution of the temperature field in the combustible material is demonstrated in Figs. (3.1.5.2) and (3.1.5.3) for a given set of fixed values for the embedded parameters. It interesting to note that the slab temperature increases gradually with time until it attains its steady state value. Generally the temperature is maximum along the slab centerline and minimum at the slab surface due to convective heat transfer to the ambient. Fig. (3.1.5.4) shows that the slab temperature is highest during bimolecular reaction ($m = 0.5$) and lowest for sensitized reaction ($m = -2$), hence confirming the earlier results in the literature [6].

In Figs. (3.1.5.5)-(3.1.5.7), we observe that the slab temperature decreases with an increase in the values of reaction order index (n), Biot number (Bi) and the oxygen consumption rate parameter (β). This clearly implies that a higher order exothermic oxidation chemical reaction will be more thermally stable than a lower one. The decrease in the slab temperature with increasing Biot number can be attributed to the action of convective cooling at the slab surface. Meanwhile, as β increases the oxygen concentration in the interior of the slab decreases leading to a decrease in the slab temperature. Figs. (3.1.5.8)-(3.1.5.9) show that the slab temperature increases with an increase in the parameter values of λ and γ . An increase in the value of Frank-Kamenetskii parameter (λ) indicates an increase in the slab internal heat generation due to exothermic oxidation reaction, this invariably leads to an elevation in the slab temperature. Moreover, since oxygen is needed and very essential for this exothermic chemical reaction, an increase in the parameter value of γ implies an increase in the supply of oxygen from the ambient to support the reaction process, leading to more internal heat been generated in the system and high temperature of the slab.

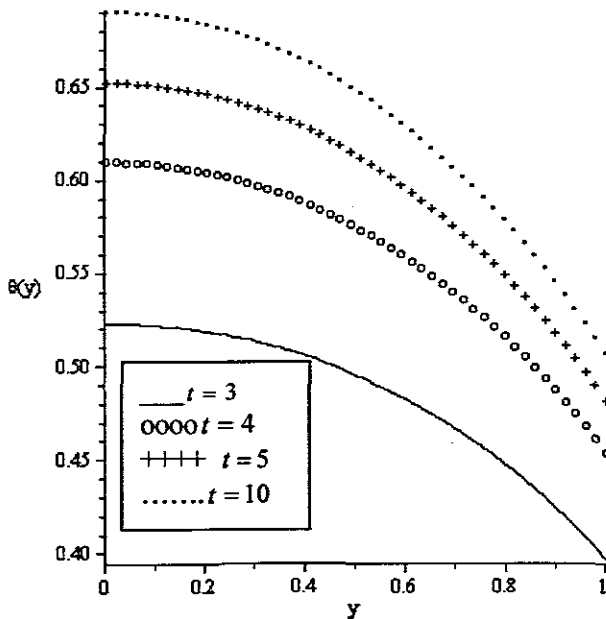


Fig. 3.1.5.2. Temperature profiles for $m=0.5$, $n=2$, $\alpha=\beta=\lambda=\gamma=Bi=1$, $\theta_a=\varepsilon=0.1$

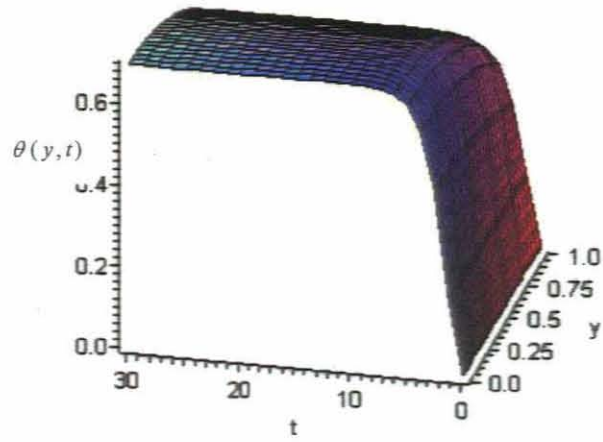


Fig. 3.1.5.3. Three dimensional plot for temperature profiles for $m=0.5$, $n=2$, $\alpha=\beta=\lambda=\gamma=Bi=1$, $\theta_a=\varepsilon=0.1$

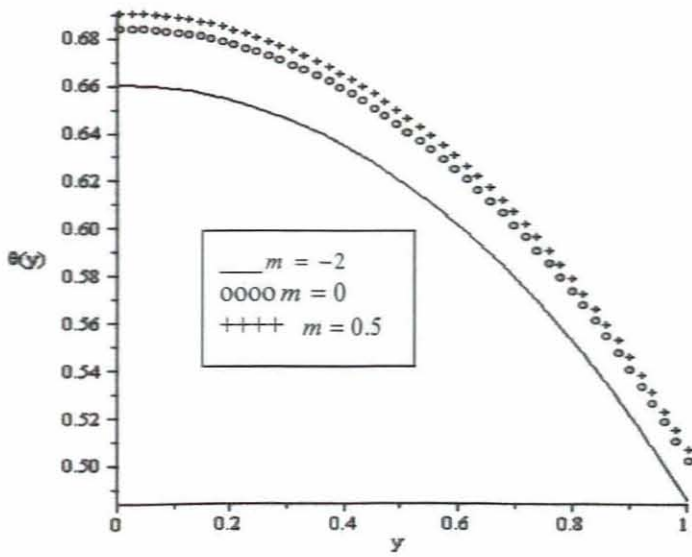


Fig. 3.1.5.4. Temperature profiles for $t=10$, $n=2$, $\alpha=\beta=\lambda=\gamma=Bi=1$, $\theta_a=\varepsilon=0.1$

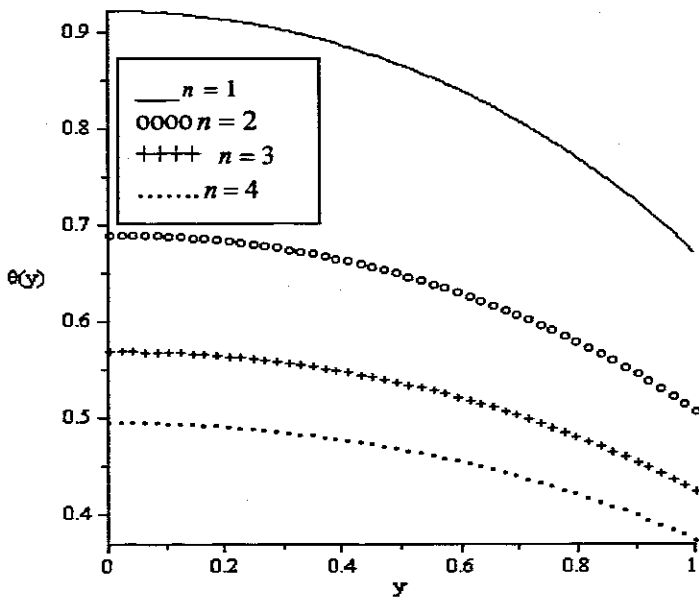


Fig. 3.1.5.5. Temperature profiles for $t = 10$, $m=0.5$, $\alpha=\beta=\lambda=\gamma=Bi=1$, $\theta_a=\epsilon=0.1$

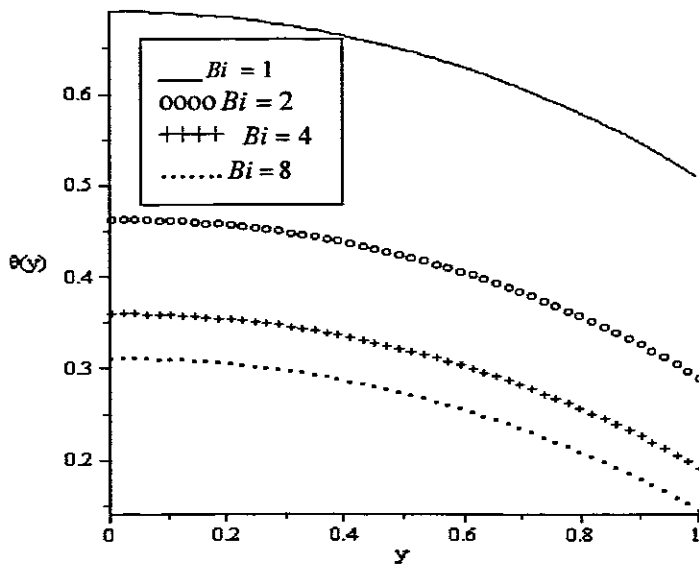


Fig. 3.1.5.6. Temperature profiles for $t = 10$, $m=0.5$, $n=2$, $\alpha=\beta=\lambda=\gamma=1$, $\theta_a=\epsilon=0.1$

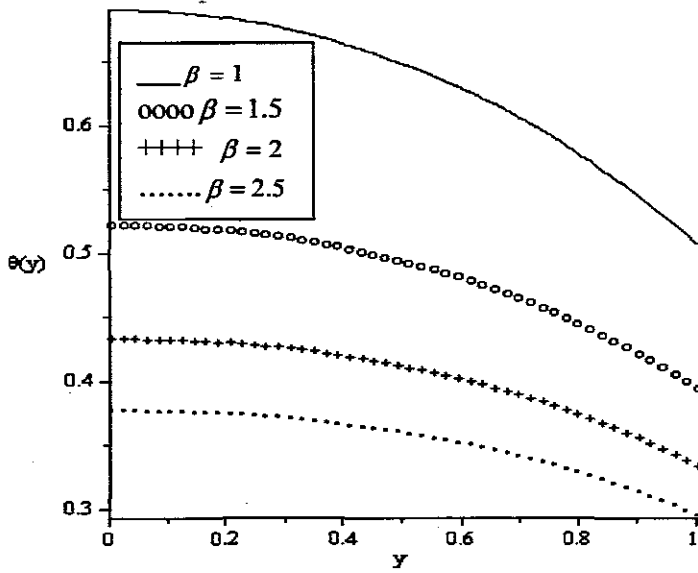


Fig. 3.1.5.7. Temperature profiles for $t = 10$, $m = 0.5$, $n = 2$, $\alpha = \gamma = \lambda = Bi = 1$, $\theta_a = \varepsilon = 0.1$

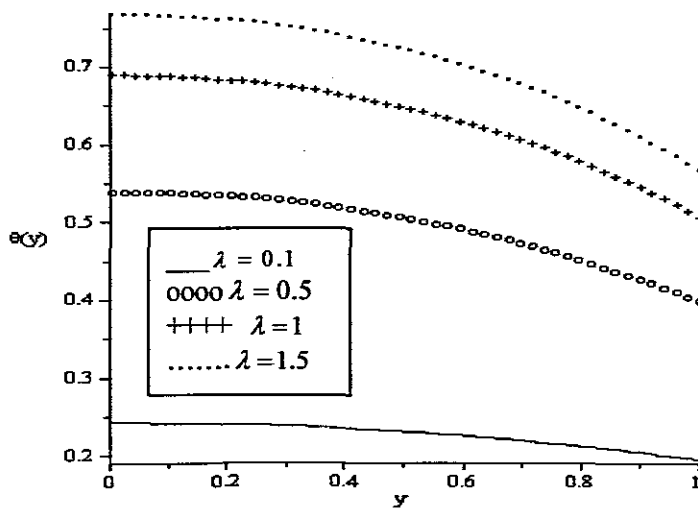


Fig. 3.1.5.8. Temperature profiles for $t = 10$, $n = 2$, $m = 0.5$, $\alpha = \beta = \gamma = Bi = 1$, $\theta_a = \varepsilon = 0.1$

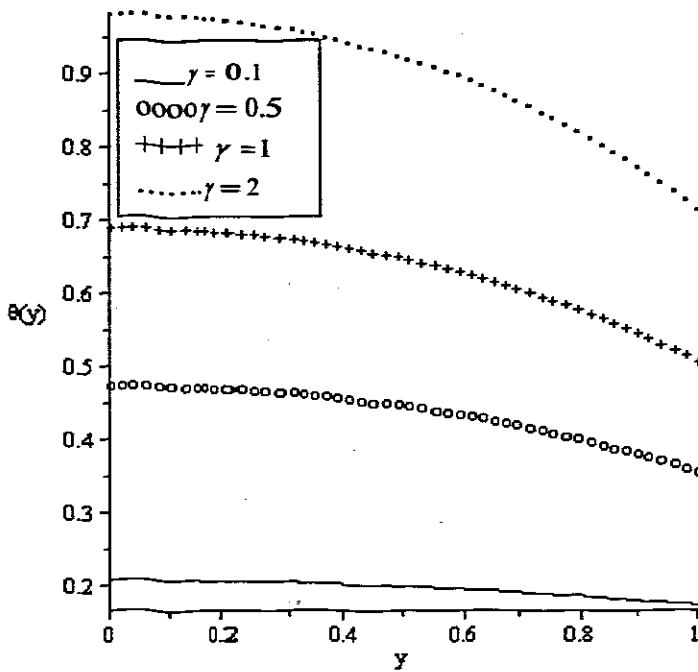


Fig. 3.1.5.9. Temperature profiles for $t=10, m=0.5, n=2, \alpha=\beta=\lambda=Bi=1, \theta_a=\epsilon=0.1$

B. Effect of various parameters on Oxygen concentration profiles

Typical curves showing the oxygen concentration profiles with the slab for different values physical parameters are shown in Figs. (3.1.5.10)-(3.1.5.17). Generally, oxygen concentration is lowest along slab centerline and attained its maximum value at the slab surface due to the transfer of oxygen at the slab surface with its surrounding. The time evolution of the oxygen concentration in the combustible material is demonstrated in Figs. (3.1.5.10) and (3.1.5.11) for a given set of fixed values for the embedded parameters. It is noteworthy that the oxygen concentration in the slab decreases gradually with time until it attains its steady state value. Fig. (3.1.5.12) shows that the oxygen concentration in the slab is lowest during bimolecular reaction ($m = 0.5$) and highest for sensitized reaction ($m = -2$). This can be attributed to the fact that oxygen consumption within the slab is highest during bimolecular chemical reaction leading to large internal heat generation and high depletion in oxygen concentration. In Figs. (3.1.5.13)-(3.1.5.15), we observe that the oxygen concentration in the slab increases with an increase in the values of reaction order index (n), Biot number (Bi) and the slab surface oxygen supply rate parameter (γ). This implies that less oxygen is consumed in the system during a higher order

exothermic oxidation chemical reaction, leading to a high level of oxygen concentration in the system than that of a lower reaction order. The increase in the oxygen concentration with increasing values Biot number and slab surface oxygen transfer parameter can be attributed to the combined effect of convective cooling and continuous supply of oxygen from the ambient at the slab surface. Figs. (3.1.5.16)-(3.1.5.17) show that the oxygen concentration in the slab decreases with an increase in the parameter values of λ and β . As Frank-Kamenetskii parameter (λ) increases, more oxygen is consumed to support high rate of chemical reaction, this invariably leads to a depletion in the slab oxygen concentration. Similarly, an increase in the parameter value of β implies an increase oxygen consumption, leading to a decrease in the slab oxygen concentration.

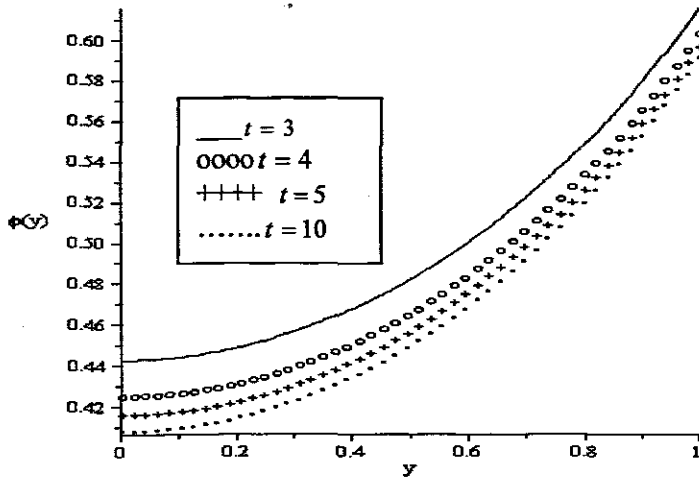


Fig. 3.1.5.10. Oxygen concentration profiles for $m=0.5$, $n=2$, $\alpha=\beta=\lambda=\gamma=Bi=1$, $\theta_a=\epsilon=0.1$

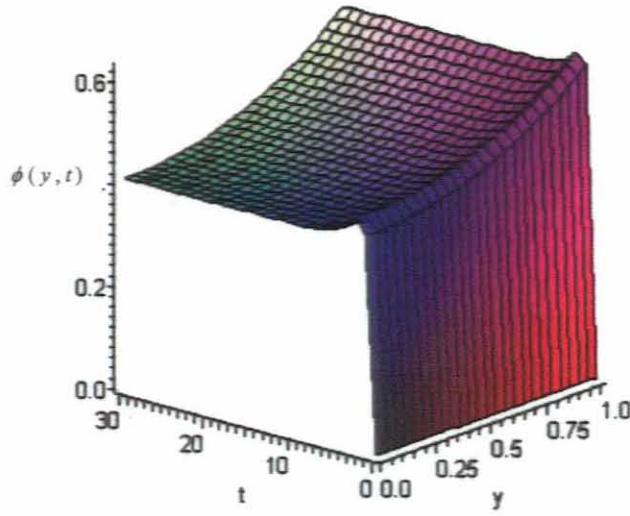


Fig. 3.1.5.11. Three dimensional plot for Oxygen concentration profiles for $m=0.5$, $n=2$, $\alpha=\beta=\lambda=\gamma=Bi=1$, $\theta_a=\varepsilon=0.1$

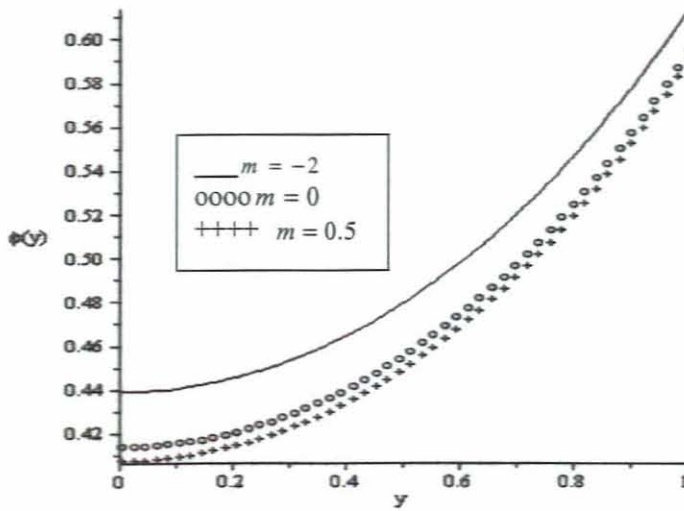


Fig. 3.1.5.12. Oxygen concentration profiles for $t = 10$, $n=2$, $\alpha=\beta=\lambda=\gamma=Bi=1$, $\theta_a=\varepsilon=0.1$

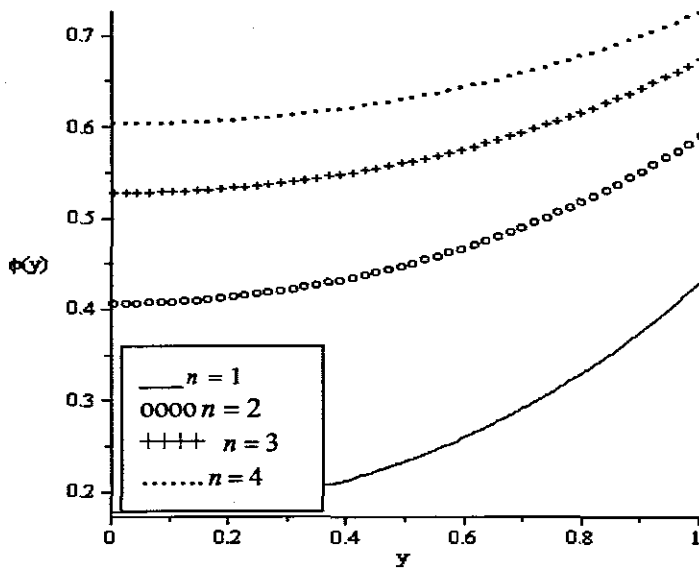


Fig. 3.1.5.13. Oxygen concentration profiles for $t=10$, $m=0.5$, $\alpha=\beta=\lambda=\gamma=Bi=1$, $\theta_a=\varepsilon=0.1$

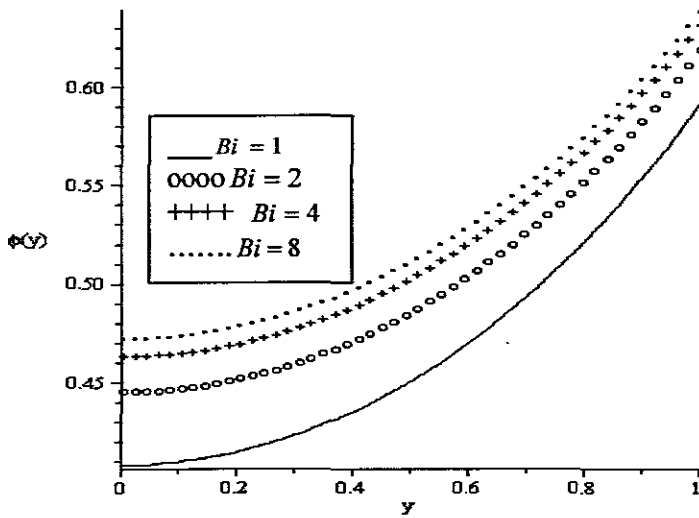


Fig. 3.1.5.14. Oxygen concentration profiles for $t=10$, $m=0.5$, $n=2$, $\alpha=\beta=\lambda=\gamma=1$, $\theta_a=\varepsilon=0.1$

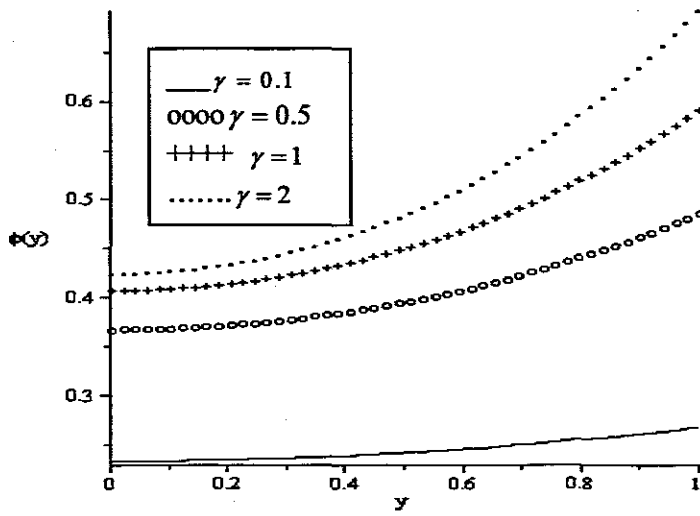


Fig. 3.1.5.15. Oxygen concentration profiles for $t=10, m=0.5, n=2,$
 $\alpha=\beta=\lambda=Bi=1, \theta_a=\varepsilon=0.1$

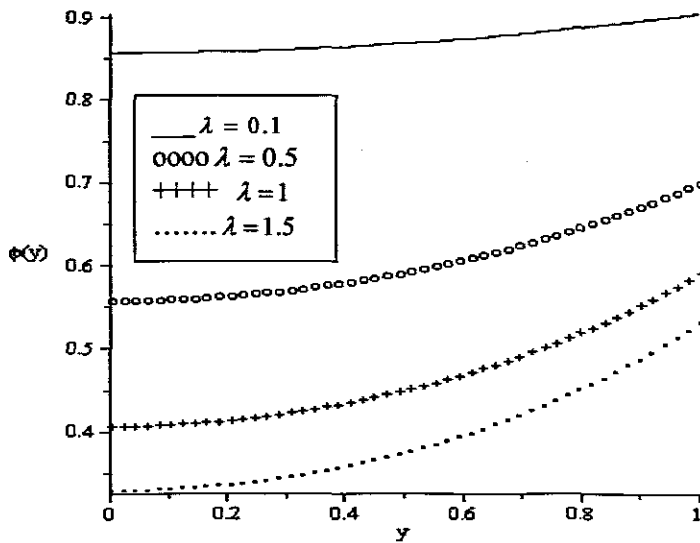


Fig. 3.1.5.16. Oxygen concentration profiles for $t=10, n=2, m=0.5,$
 $\alpha=\beta=\gamma=Bi=1, \theta_a=\varepsilon=0.1$

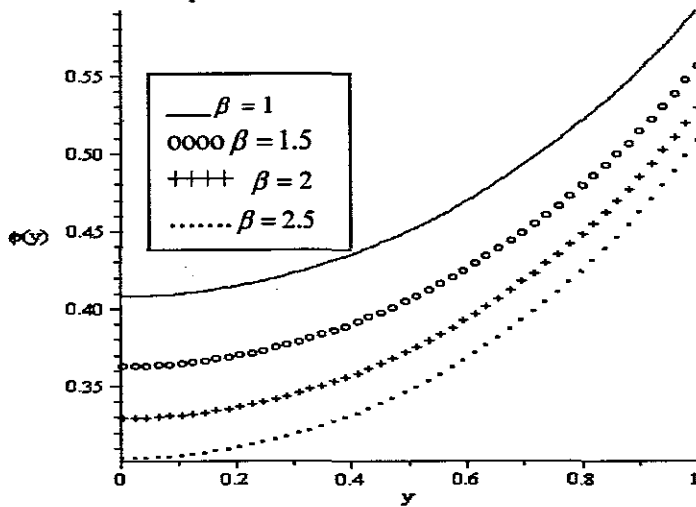


Fig. 3.1.5.17. Oxygen concentration profiles for $t=10$, $m=0.5$, $n=2$, $\alpha=\gamma=\lambda=Bi=1$, $\theta_a=\varepsilon=0.1$.

3.1.6. Conclusion

In this paper an analysis has been carried out to study the thermal development in a combustible material under a one-step exothermic oxidation n th order chemical reaction, taking the diffusion and consumption of the reactant into account. The pre-exponential factor is assumed to be temperature dependent and the nonlinear partial differential equations governing the transient problem are solved numerically using *semi-discretization technique called method of lines*. The effects of various embedded parameters on the system are displayed graphically. Our results reveal among others, that the internal heat generation in the system decreases while the oxygen concentration increases with an increase in the parameter values of reaction order index (n) and Biot number (Bi). Furthermore, it is noteworthy that the slab temperature is highest while the oxygen concentration is lowest during bimolecular reaction in comparison to Arrhenius and sensitized types of chemical reaction.

4.1. Analysis of steady state exothermic reaction in a slab with convective boundary conditions

4.1.1. Summary

In this chapter, we considered a steady state, exothermic n th order chemical reaction in a slab with reactant consumption in the presence of convective heat and oxygen exchange with the surrounding ambient at the slab surface. The coupled nonlinear differential equations governing the system are obtained and solved using perturbation technique and together with a special type of Hermite-Padé series summation and improvement method. Important properties of the temperature field including the effects of embedded parameters on the thermal stability of the system are discussed.

4.1.2. Introduction

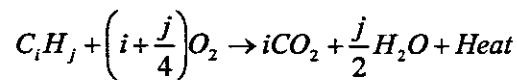
Study of thermal stability of a reactive chemical aimed at ensuring the safety of its storage, transportation and use is an important practical aspect of reactive hazard assessment. This study focuses on determination of critical conditions that separate explosive and non-explosive domains of a proceeding reaction and evaluation of induction period of an explosion if it appears. Two main approaches are used for obtaining the necessary data. They are based either on direct determination of the explosion characteristics by means of explosive experiments or on application of theoretical calculations. One of the most important advantages of theoretical methods is that they can be applied as soon as a kinetic model had been evaluated from data from laboratory scale kinetic experiments. In particular, they allow estimation of runaway parameters in the earliest stages of the life cycle of a chemical product, thus ensuring elimination or significant reduction of the necessity for explosive experiments. The approach based on the mathematical combustion theory, in its turn, unites two branches—the family of semi-analytical methods and more sophisticated numerical simulation methods. The grounds for the semi-analytical simplified theories developed by Semenov [1], Frank-Kamenetskii [2] and others are well known. They give convenient approximate analytical relations that do not require complicated

calculations and are currently used as a rule for estimation of critical parameters. However, the application domain of these theories is essentially limited; therefore many practical problems cannot be solved without applying comprehensive models that require the use of numerical calculations. This approach will be referred to as the simulation-based approach.

Although thermal explosion has received much attention in the literature, the vast majority of investigations have been concerned with homogeneous boundary conditions ranging from the infinite Biot number case of a constant surface temperature (Frank-Kamenetskii conditions) through a range of Biot numbers to zero (Semenov conditions). The studies have included a variety of geometries and have been directed towards obtaining critical conditions for thermal ignition to occur, in the form of a critical value for the Frank-Kamenetskii parameter. The present investigation aims to reconsider these problems providing a fuller study of thermal stability of a reacting slab with reactant consumption in the presence of convective heat and oxygen exchange with the ambient at the slab surface.

4.1.3. Mathematical model

The geometry of the problem is depicted in Fig. (4.1.3.1) It is assumed that the combustible material is undergoing an n th order oxidation chemical reaction. The complicated chemistry involved in the problem is simplified by assuming a one-step finite-rate irreversible reaction between the combustible material (hydrocarbon) and the oxygen of the air i.e.,



[Combustible material + Oxygen → Heat + Carbondioxide + Water]

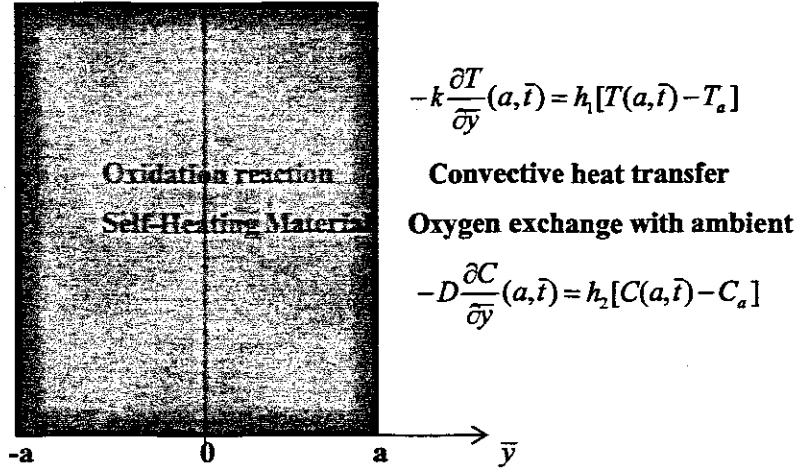


Fig. 4.1.3.1: Geometry of the Problem

Following [6, 13, 14], the nonlinear partial differential equations describing the temperature and oxygen concentration in the combustible material can be written as;

$$k \frac{d^2 T}{d\bar{y}^2} + QA \left(\frac{KT}{l} \right)^m (C - C_0)^n e^{\frac{E}{RT}} = 0, \quad (4.1.3.1)$$

$$D \frac{d^2 C}{d\bar{y}^2} - A \left(\frac{KT}{l} \right)^m (C - C_0)^n e^{\frac{E}{RT}} = 0, \quad (4.1.3.2)$$

with boundary conditions as

$$-k \frac{dT}{d\bar{y}} = h_1 [T - T_a], \quad -D \frac{dC}{d\bar{y}} = h_2 [C - C_a], \quad \text{at } \bar{y} = a, \quad (4.1.3.3)$$

$$\frac{dT}{d\bar{y}} = \frac{dC}{d\bar{y}} = 0, \quad \bar{y} = 0, \quad (4.1.3.4)$$

where T is the absolute temperature, T_a is the ambient temperature, C_a is the oxygen concentration in the surrounding air, C_0 is the initial concentration of oxygen in the material, T_0 is the slab initial temperature, k is the thermal conductivity of the material, Q is the exothermicity, A is the rate constant, E is the activation energy, R is the universal gas constant, l is the Planck's number, K is the Boltzmann's constant, ν is the vibration frequency, a is the slab half width, \bar{y} is the distance measured

transverse direction, h_1 is the heat transfer between the material and its surroundings, D is the diffusivity of oxygen in the material, h_2 is the transfer of oxygen from the material to its surroundings, n is the chemical reaction order and m is the numerical exponent such that $m = \{-2, 0, \frac{1}{2}\}$ represent numerical exponent for Sensitised, Arrhenius and Bimolecular kinetics respectively (see [1, 6]). We introduce the following dimensionless variables into Eqs. (4.1.3.1)- (4.1.3.4)

$$Bi = \frac{h_1 a}{k}, \gamma = \frac{h_2 a}{D}, \phi = \frac{(C - C_0)}{(C_a - C_0)}, \theta = \frac{E(T - T_0)}{RT_0^2}, \theta_a = \frac{E(T_a - T_0)}{RT_0^2}, y = \frac{\bar{y}}{a}, \quad (4.1.3.5)$$

$$\varepsilon = \frac{RT_0}{E}, \alpha = \frac{k}{D\rho c_p}, \lambda = \frac{QAEa^2(C_a - C_0)^n \left[\frac{KT_0}{\omega} \right]^m e^{\frac{E}{RT_0}}}{kRT_0^2}, \beta = \frac{kRT_0^2}{DQE(C_a - C_0)},$$

and we obtain the dimensionless governing equations as

$$\frac{d^2 \theta}{dy^2} + \lambda(1 + \varepsilon \theta)^m \phi^n e^{\frac{\theta}{1 + \varepsilon \theta}} = 0, \quad (4.1.3.6)$$

$$\frac{d^2 \phi}{dy^2} - \lambda \beta (1 + \varepsilon \theta)^m \phi^n e^{\frac{\theta}{1 + \varepsilon \theta}} = 0, \quad (4.1.3.7)$$

and the associated boundary conditions (4.1.3.3)-(4.1.3.4) become

$$\frac{d\theta}{dy} = -Bi[\theta - \theta_a], \quad \frac{d\phi}{dy} = -\gamma[\phi - 1] \quad \text{at } y = 1 \quad (4.1.3.8)$$

$$\frac{d\theta}{dy} = \frac{d\phi}{dy} = 0, \quad \text{at } y = 0 \quad (4.1.3.9)$$

where $\lambda, \varepsilon, \beta, \gamma, Bi$ represent the Frank-Kamenetskii parameter, activation energy parameter, Oxygen consumption rate parameter, mass Biot number and the thermal Biot number respectively. A body of material releasing heat to its surroundings may achieve a safe steady-state where the temperature of the body reaches some moderate value and stabilizes. However, when the rate of heat generation of the material exceeds the rate of heat loss to the surroundings, then ignition can occur. In the following section, equations (4.1.3.6) - (4.1.3.9) are solved using perturbation method.

4.1.4. Perturbation Method

Due to the nonlinear nature of the temperature and reacting species concentration equations in (4.1.3.6) and (4.1.3.7), it is convenient to seek a solution in the form a power series expansion in parameter λ i.e.

$$\theta = \sum_{i=0}^{\infty} \theta_i \lambda, \quad \phi = \sum_{i=0}^{\infty} \phi_i \lambda \quad (4.1.4.1)$$

Substituting the solution series in equation (4.1.4.1) into equations (4.1.3.6) - (4.1.3.9) and collecting the coefficients of like powers of λ , we obtained the followings:

Order zero (λ^0)

$$\frac{d^2\theta_0}{dy^2}=0, \quad \frac{d^2\phi_0}{dy^2}=0$$

$$\text{with } \frac{d\theta_0}{dy}(1) = -Bi[\theta_0(1) - \theta_a], \quad \frac{d\phi_0}{dy}(1) = -\gamma[\phi_0(1) - 1], \quad \frac{d\theta_0}{dy}(0) = \frac{d\phi_0}{dy}(0) = 0,$$

Order one (λ^1)

$$\frac{d^2\theta_1}{dy^2} = -(1 + \varepsilon\theta_0)^m \phi_0^n e^{\frac{\theta_0}{(1+\varepsilon\theta_0)}},$$

$$\frac{d^2\phi_1}{dy^2} = \beta(1 + \varepsilon\theta_0)^m \phi_0^n e^{\frac{\theta_0}{(1+\varepsilon\theta_0)}} = 0,$$

with

$$\frac{d\theta_1}{dy}(1) = -Bi\theta_1(1), \quad \frac{d\phi_1}{dy}(1) = -\gamma\phi_1(1), \quad \frac{d\theta_1}{dy}(0) = \frac{d\phi_1}{dy}(0) = 0$$

Order two (λ^2)

$$\frac{d^2\theta_2}{dy^2} = -(1 + \varepsilon\theta_0)^m \phi_0^n e^{\frac{\theta_0}{(1+\varepsilon\theta_0)}} \left[\frac{\theta_1}{(1 + \varepsilon\theta_0)^2} + n \frac{\phi_1}{\phi_0} + \frac{m\varepsilon\theta_1}{(1 + \varepsilon\theta_0)} \right],$$

$$\frac{d^2\phi_2}{dy^2} = \beta(1 + \varepsilon\theta_0)^m \phi_0^n e^{\frac{\theta_0}{(1+\varepsilon\theta_0)}} \left[\frac{\theta_1}{(1 + \varepsilon\theta_0)^2} + n \frac{\phi_1}{\phi_0} + \frac{m\varepsilon\theta_1}{(1 + \varepsilon\theta_0)} \right],$$

with

$$\frac{d\theta_2}{dy}(1) = -Bi\theta_2(1), \quad \frac{d\phi_2}{dy}(1) = -\gamma\phi_2(1), \quad \frac{d\theta_2}{dy}(0) = \frac{d\phi_2}{dy}(0) = 0$$

and so on. The above equations for the coefficients of solution series are solved iteratively for the temperature fields and reacting species concentration, we obtain;

$$\theta(y) = \theta_a - \frac{\lambda}{2Bi} (1 + \varepsilon\theta_a)^m e^{\frac{\theta_a}{1 + \varepsilon\theta_a}} (y^2 Bi - 2 - Bi) + O(\lambda^2) \quad (4.1.4.2)$$

$$\phi(y) = 1 + \frac{\lambda\beta}{2\gamma} (1 + \varepsilon\theta_a)^m e^{\frac{\theta_a}{1 + \varepsilon\theta_a}} (y^2 \gamma - 2 - \gamma) + O(\lambda^2) \quad (4.1.4.3)$$

Using a computer symbolic algebra package (MAPLE), the first few terms of the above solution series in Eqs. (4.1.4.2) - (4.1.4.3) are obtained. We are aware that

these power series solutions are valid for very small parameter values of λ . However, using Hermite-Padé series summation and improvement technique, we have extended the usability of the solution series beyond small parameter values as illustrated in the following section.

4.1.5. Hermite-Padé Approximation Technique

From the application point of view, it is very important to determine the appearance of criticality or non-existence of steady-state solution for certain parameter values. In order to achieve this, we first derived a special type of Hermite-Padé approximant. Let

$$U_N(\lambda) = \sum_{n=0}^N a_n \lambda^n + O(\lambda^{N+1}), \quad \text{as } \lambda \rightarrow 0, \quad (4.1.5.1)$$

be a given partial sum. It is important to note here that Eq. (4.1.5.1) can be used to approximate any output of the solution of the problem under investigation (e.g. the series for the wall heat flux parameter in terms of Nusselt number $Nu = -d\theta/dy$ at $y = 1$), since everything can be Taylor expanded in the given small parameter. Assume $U(\lambda)$ is a local representation of an algebraic function of λ in the context of nonlinear problems, we seek an expression of the form

$$F_d(\lambda, U) = \sum_{m=1}^d \sum_{k=0}^m f_{m-k,k} \lambda^{m-k} U^k, \quad (4.1.5.2)$$

of degree $d \geq 2$, such that

$$\frac{\partial F_d}{\partial U}(0,0) = 1 \text{ and } F_d(\lambda, U_N) = O(\lambda^{N+1}), \quad \text{as } \lambda \rightarrow 0. \quad (4.1.5.3)$$

The requirement (4.1.5.3) reduces the problem to a system of N linear equations for the unknown coefficients of F_d . The entries of the underlying matrix depend only on the N given coefficients a_n and we shall take $N = (d^2 + 3d - 2)/2$, so that the number of equations equals the number of unknowns. The polynomial F_d is a special type of Hermite-Padé approximant and is then investigated for bifurcation and criticality conditions using Newton diagram, Vainberg and Trenogin [36].

4.1.6. Numerical Approach

The numerical technique chosen for the solution of the coupled ordinary differential equations (4.1.3.6) and (4.1.3.7) is the standard Newton–Raphson shooting method along with a fourth-order Runge–Kutta integration algorithm. Eqs. (4.1.3.6)–(4.1.3.7) are transformed into a system of first order differential equations as follows. Let $\theta = x_1$, $\theta' = x_2$, $\phi = x_3$, $\phi' = x_4$, where the prime symbol represent derivatives with respect to y . Then, the problem becomes,

$$x_1' = x_2, \quad x_2' = -\lambda(1 + \varepsilon x_1)^m x_3^n e^{\frac{x_1}{(1+\varepsilon x_1)}}, \quad x_3' = x_4, \quad x_4' = \lambda\beta(1 + \varepsilon x_1)^m x_3^n e^{\frac{x_1}{(1+\varepsilon x_1)}} \quad (4.1.6.1)$$

subject to the following initial conditions,

$$x_1(0) = s_1, x_2(0) = 0, x_3(0) = s_2, x_4(0) = 0. \quad (4.1.6.2)$$

The unspecified initial conditions s_1 and s_2 are guessed systematically and Eq. (4.1.6.1) is then integrated numerically as initial valued problems until the given boundary conditions at $y=1$ are satisfied. For each set of parameter values for λ , ε , β , γ and Bi , the procedure is repeated until conditions at the $y = 1$ are satisfied and the desired degree of accuracy (namely 10^{-7}) of the results obtained is achieved.

4.1.7 Results and Discussion

In this section, we validate the above theoretical results using physically realistic values of various embedded parameters in the numerical experiment. It is important to note that increasing parameter value of λ indicates an increase in the rate of exothermic chemical kinetics in the slab. A comparison between the results obtained using the partial sum involving the first 20 terms of the perturbation series solution and purely fourth-order Runge–Kutta numerical integration coupled with shooting method at small and moderate values of embedded parameters are shown in Table 4.1.7.1. Generally, the difference is of order 10^{-8} and a perfect agreement is noticed.

Table 4.1.7.1: Comparison between analytical and numerical results ($\lambda=\beta=\gamma=0.1$, $\varepsilon=0$, $n=2$, $Bi=\theta_a=1$)

| y | $\theta(y)$ Perturbation Results | $\theta(y)$ Numerical Results | $ \theta_{numer.} - \theta_{perturb.} $ |
|-----|--|-------------------------------------|---|
| 0 | 1.32892926 | 1.32892929 | 3.0×10^{-8} |
| 0.1 | 1.32780785 | 1.32780788 | 3.0×10^{-8} |
| 0.2 | 1.32444550 | 1.32444553 | 3.0×10^{-8} |
| 0.3 | 1.31884776 | 1.31884779 | 3.0×10^{-8} |
| 0.4 | 1.31102389 | 1.31102392 | 3.0×10^{-8} |
| 0.5 | 1.30098675 | 1.30098677 | 2.0×10^{-8} |
| 0.6 | 1.28875273 | 1.28875276 | 3.0×10^{-8} |
| 0.7 | 1.27434168 | 1.27434170 | 2.0×10^{-8} |
| 0.8 | 1.25777674 | 1.25777676 | 2.0×10^{-8} |
| 0.9 | 1.23908423 | 1.23908425 | 2.0×10^{-8} |
| 1.0 | 1.21829349 | 1.21829351 | 2.0×10^{-8} |

In order to obtain the thermal stability criterion in the reacting slab, the Hermite-Padé approximation procedure in section (4.1.5) above was applied to the first few terms of the solution series in section (4.1.4) and we obtained the results as shown in tables (4.1.7.2) and (4.1.7.3) below:

Table 4.1.7.2: Computations showing the criticality procedure rapid convergence ($\beta = 0.1$, $\gamma = Bi = \theta_a = n = 1$, $\varepsilon = 0$).

| d | N | θ_{max} | λ_{cN} |
|-----|-----|----------------|----------------|
| 2 | 4 | 2.133563429 | 0.111399437253 |
| 3 | 8 | 2.245843906 | 0.111399418112 |
| 4 | 13 | 2.245636361 | 0.111399421506 |
| 5 | 19 | 2.245636371 | 0.111399421512 |
| 6 | 26 | 2.245636371 | 0.111399421512 |

Table 4.1.7.3: Computations showing thermal ignition criticality for different parameter values

| Bi | γ | β | n | θ_a | m | ε | θ_{max} | λ_c |
|----------|----------|---------|-----|------------|------|---------------|----------------|---------------|
| 0.1 | 1 | 0.01 | 1 | 1.0 | 0.0 | 0.00 | 2.0172018519 | 0.01310984287 |
| 1 | 1 | 0.01 | 1 | 1.0 | 0.0 | 0.00 | 2.1163034602 | 0.10058516043 |
| 10 | 1 | 0.01 | 1 | 1.0 | 0.0 | 0.00 | 2.2127440013 | 0.27532575932 |
| 100 | 1 | 0.01 | 1 | 1.0 | 0.0 | 0.00 | 2.2200715856 | 0.32658480960 |
| ∞ | 1 | 0.01 | 1 | 1.0 | 0.0 | 0.00 | 2.2205606260 | 0.33330414740 |
| 1 | 5 | 0.01 | 1 | 1.0 | 0.0 | 0.00 | 2.1098592062 | 0.09999778812 |
| 1 | 10 | 0.01 | 1 | 1.0 | 0.0 | 0.00 | 2.1090640021 | 0.09992508139 |
| 1 | 1 | 0.05 | 1 | 1.0 | 0.0 | 0.00 | 2.1666489097 | 0.10496770865 |
| 1 | 1 | 0.10 | 1 | 1.0 | 0.0 | 0.00 | 2.2456363719 | 0.11139942151 |
| 1 | 1 | 0.01 | 3 | 1.0 | 0.0 | 0.00 | 2.1395726916 | 0.10267041887 |
| 1 | 1 | 0.01 | 5 | 1.0 | 0.0 | 0.00 | 2.1638439062 | 0.10484446876 |
| 1 | 1 | 0.01 | 1 | 0.5 | 0.0 | 0.00 | 1.6163034602 | 0.16583689354 |
| 1 | 1 | 0.01 | 1 | 0.1 | 0.0 | 0.00 | 1.2163034602 | 0.24739957357 |
| 1 | 1 | 0.01 | 1 | 1.0 | 0.0 | 0.01 | 2.1633708697 | 0.10474696724 |
| 1 | 1 | 0.01 | 1 | 1.0 | 0.5 | 0.01 | 2.1572733201 | 0.10368955515 |
| 1 | 1 | 0.01 | 1 | 1.0 | -2.0 | 0.01 | 2.1884248614 | 0.10911552331 |
| 1 | 1 | 0.01 | 1 | 1.0 | 0.0 | 0.10 | 2.7942887760 | 0.15217860387 |

The results in table (4.1.7.2) reveal the rapid convergence of Hermite-Padé approximation procedure with gradual increase in the number of series coefficients utilized in the approximants. In table (4.1.7.3), it is noteworthy that the magnitude of thermal ignition criticality (λ_c) increases with an increase the thermal Biot number ($Bi > 0$) due to convective cooling and a decrease in the oxygen supply from the surrounding ambient represented by a decrease in parameter value of γ . This invariably will lead to a delay in the development of thermal runaway in the reacting slab and enhances thermal stability. Similar effect of thermal stability enhancement is observed with increasing parameter values of β , n , ε and a decrease in the value of ambient temperature parameter θ_a . Thus, higher order oxidation chemicals kinetic

augment thermal stability. It is worth mentioning that a combined increase in the parameter values of γ , θ_a and decrease in the parameter values of Bi , β , n , ε can cause a decrease in the magnitude of thermal criticality parameter (λ), leading to early development of thermal ignition in the system. Furthermore, it is interesting to note from table (4.1.7.3) that thermal ignition occur faster in a bimolecular ($m=0.5$) type of exothermic oxidation reaction as compared to the Arrhenius ($m=0$) and sensitised ($m=-2$) type of reaction. A slice of the bifurcation diagram for $0 \leq \varepsilon \ll 1$ in the (λ, θ_{max}) plane is shown in Fig. (4.1.7.1). It represents the qualitative change in the thermal system as the parameter (λ) increases. In particular, for $0 \leq \varepsilon \ll 1$, $Bi > 0$, $\beta > 0$, $\gamma > 0$ and $n > 0$, there is a critical value λ_c (a turning point) such that, for $0 < \lambda < \lambda_c$ there are two solutions (labelled I and II). The upper and lower solution branches occur due to the nonlinearity in the temperature dependent chemical kinetics in the governing equations for energy and concentration balance. When $\lambda > \lambda_c$ the system has no real solution and displays a classical form indicating thermal runaway. As exothermic reaction due to oxidation chemical kinetics increases, the slab temperature increases uncontrollably until it ignites.

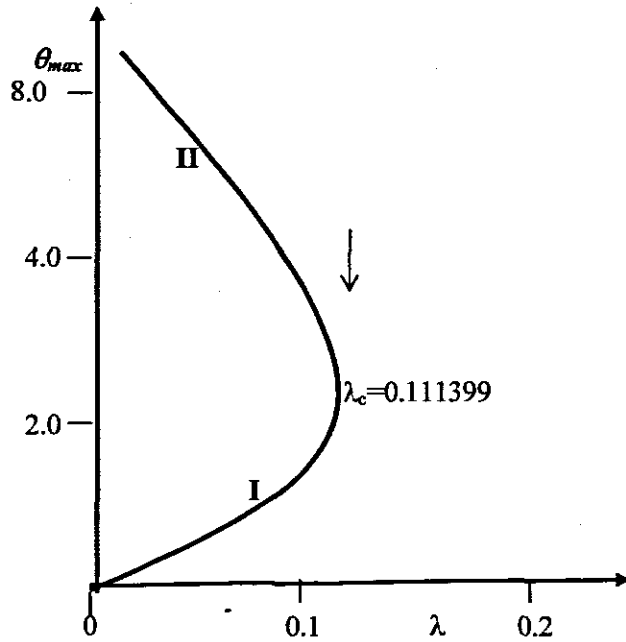


Fig. 4.1.7.1. A slice of approximate bifurcation diagram in the (λ, θ_{max}) plane when $\beta = 0.1, \varepsilon = 0, \gamma = Bi = \theta_a = n = 1$.

A. Effect of various parameters on temperature profiles

Figs. (4.1.7.2)-(4.1.7.7) illustrate the effects of various thermophysical parameters on the steady state slab temperature profiles. The temperature is maximum along the slab centerline and minimum at the slab surface due to convective heat transfer to the ambient. Fig. (4.1.7.2) shows that the slab temperature is highest during bimolecular reaction ($m = 0.5$) and lowest for sensitized reaction ($m = -2$), hence confirming the earlier results in the literature [6]. This observation is also in agreement with the results highlighted in table (4.1.7.3). In Figs. (4.1.7.3)-(4.1.7.5), we observe that the slab temperature decreases with an increase in the values of reaction order index (n), Biot number (Bi) and the oxygen consumption rate parameter (β). This confirms the results in table (4.1.7.3) that a higher order exothermic oxidation chemical reaction will be more thermally stable than a lower one. The decrease in the slab temperature with increasing Biot number can be attributed to the action of convective cooling at the slab surface. As β increases the oxygen concentration in the interior of the slab decreases leading to a decrease in the slab temperature. Figs. (4.1.7.6)-(4.1.7.7) show

that the slab temperature increases with an increase in the parameter values of λ and γ . As the Frank-Kamenetskii parameter (λ) increases, the slab internal heat generation due to exothermic oxidation reaction increases, this invariably leads to an elevation in the slab temperature. An increase in the parameter value of γ implies an increase in the supply of oxygen from the ambient to support the reaction process (since oxygen is needed and very essential for this exothermic chemical reaction), leading to more internal heat been generated in the system and high temperature of the slab.

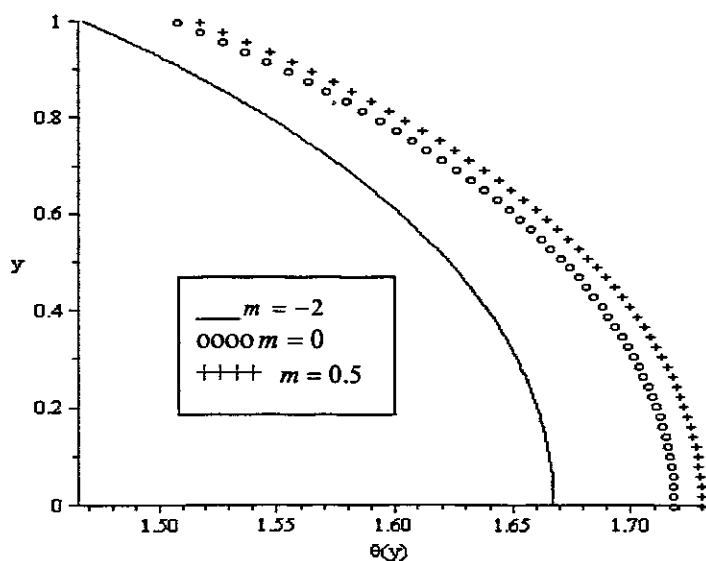


Fig.4.1.7.2. Temperature profiles for $n = 2$, $\beta = \lambda = \gamma = Bi = \theta_a = 1$, $\varepsilon = 0.1$

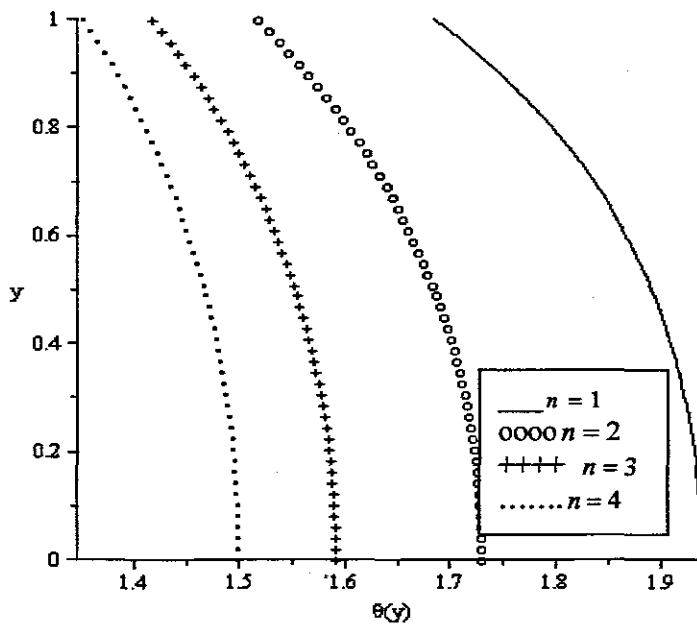


Fig.4.1.7.3. Temperature profiles for $m=0.5$, $\beta=\lambda=\gamma=Bi=\theta_a=1$, $\epsilon=0.1$

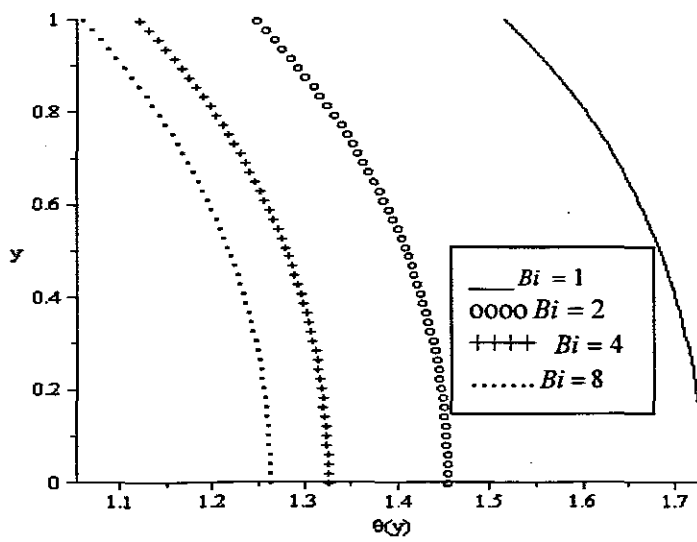


Fig.4.1.7.4. Temperature profiles for $n=2$, $m=0.5$, $\beta=\lambda=\gamma=\theta_a=1$, $\epsilon=0.1$

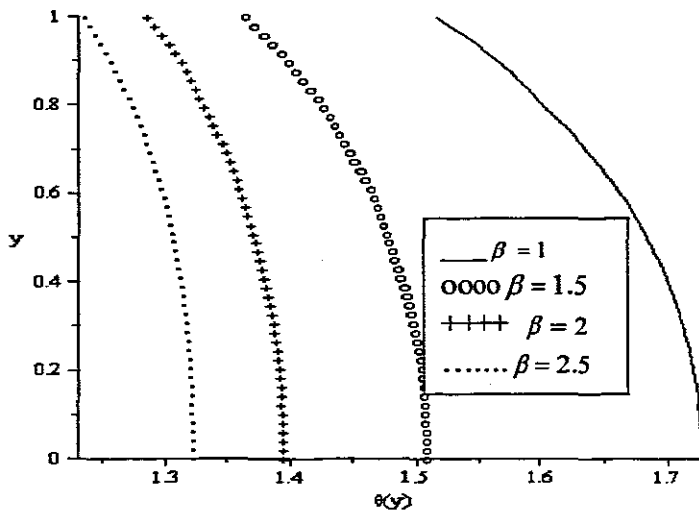


Fig.4.1.7.5. Temperature profiles for $n = 2, m=0.5, \lambda=Bi=\gamma=\theta_a=1, \epsilon=0.1$

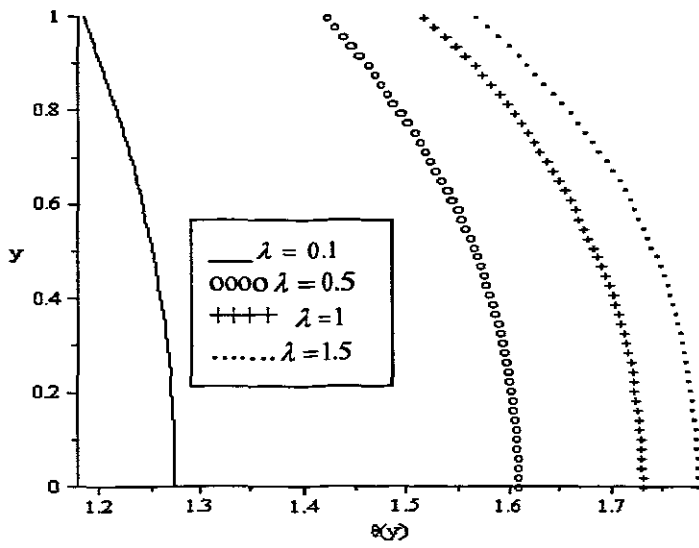


Fig.4.1.7.6. Temperature profiles for $n = 2, m=0.5, \beta=Bi=\gamma=\theta_a=1, \epsilon=0.1$

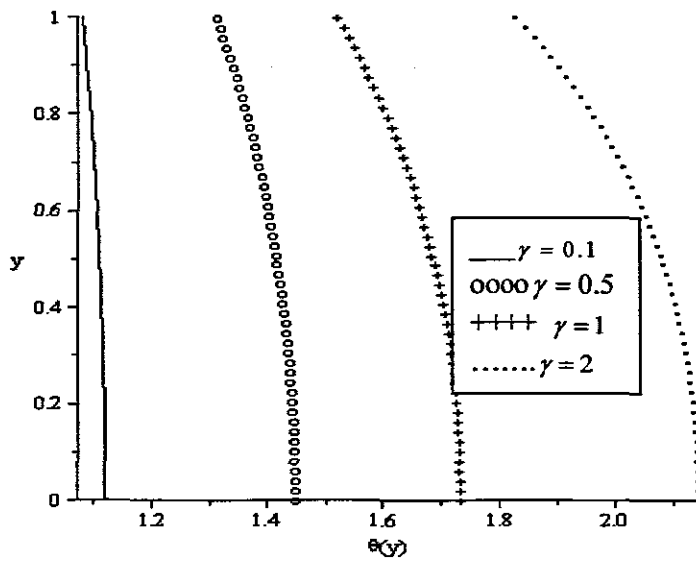


Fig.4.1.7.7. Temperature profiles for $n = 2, m=0.5, \beta=Bi=\lambda=\theta_a=1, \epsilon=0.1$

B. Effect of various parameters on Oxygen concentration profiles

Figs. (4.1.7.8)-(4.1.7.13) illustrate the oxygen concentration profiles within the slab for different values of physical parameters. The concentration of oxygen is lowest along slab centerline and highest at the slab surface due to exchange of oxygen at the slab surface with its surrounding ambient. Fig. (4.1.7.8) shows that the oxygen concentration in the slab is lowest during bimolecular reaction ($m = 0.5$) and highest for sensitized reaction ($m = -2$). This can be attributed to the fact that oxygen consumption within the slab is highest during bimolecular chemical reaction leading to large internal heat generation and high depletion in oxygen concentration. In Figs. (4.1.7.9)-(4.1.7.11), we observe that the oxygen concentration in the slab increases with an increase in the values of reaction order index (n), Biot number (Bi) and the slab surface oxygen supply rate parameter (γ). This implies that less oxygen is consumed in the system during a higher order exothermic oxidation chemical reaction, leading to a high level of oxygen concentration in the system than that of a lower reaction order. The increase in the oxygen concentration with increasing values Biot number and slab surface oxygen transfer parameter can be attributed to the combined effect of convective cooling and continuous supply of oxygen from the ambient at the slab surface. Figs. (4.1.7.12)-(4.1.7.13) show that the oxygen

concentration in the slab decreases with an increase in the parameter values of λ and β . As Frank-Kamenetskii parameter (λ) increases, more oxygen is consumed to support high rate of chemical reaction, this invariably leads to a depletion in the slab oxygen concentration. Similarly, as parameter value of β increases, oxygen consumption increases, leading to a decrease in the slab oxygen concentration.

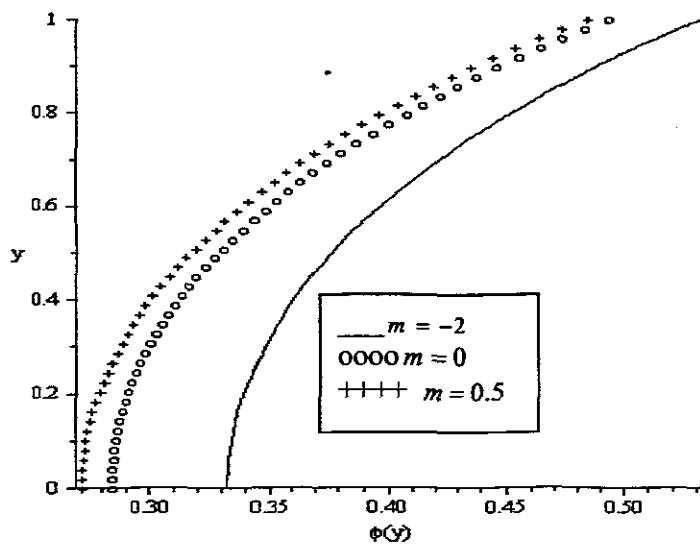


Fig4.1.7.8. Oxygen concentration profiles for $n=2$, $\beta=\lambda=\gamma=Bi=\theta_a=1$, $\epsilon=0.1$

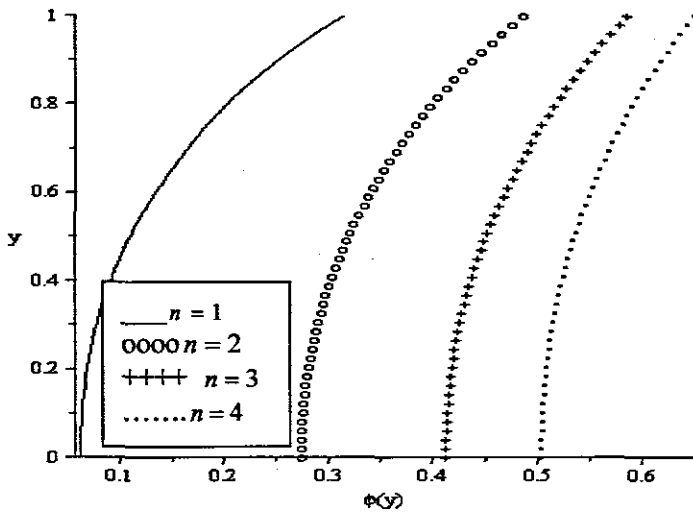


Fig.4.1.7.9. Oxygen concentration profiles for $m=0.5$, $\beta=\lambda=\gamma=Bi=\theta_a=1$, $\varepsilon=0.1$

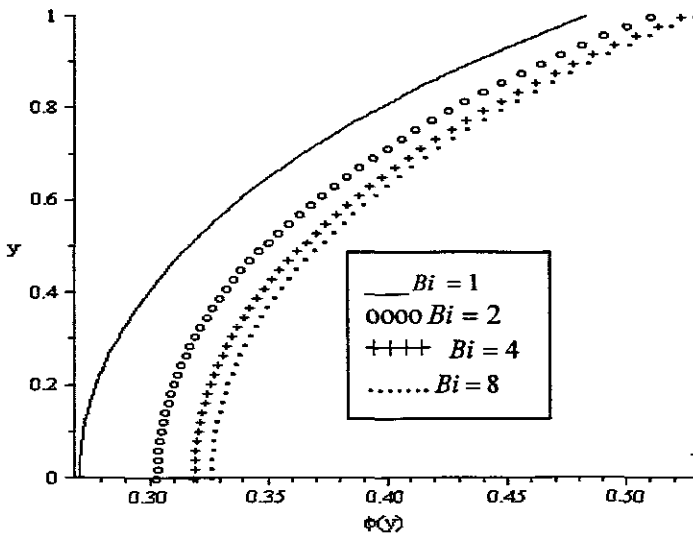


Fig.4.1.7.10. Oxygen concentration profiles for $n=2$, $m=0.5$, $\beta=\lambda=\gamma=\theta_a=1$, $\varepsilon=0.1$

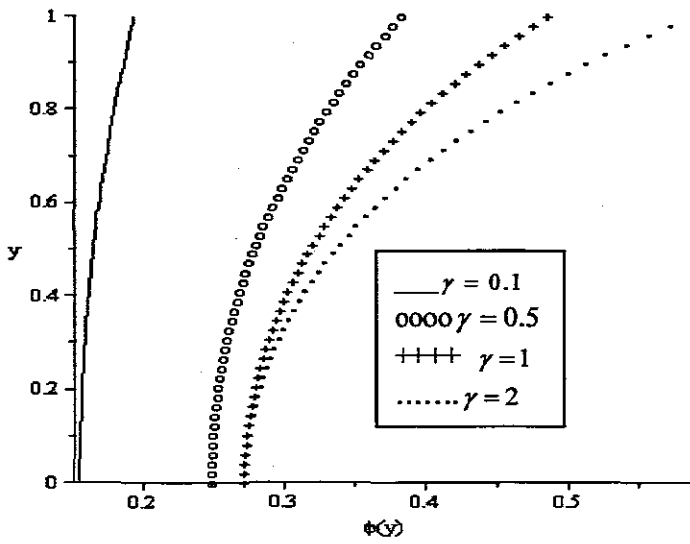


Fig.4.1.7.11. Oxygen concentration profiles for $n = 2, m=0.5, \beta=Bi=\lambda=\theta_a=1, \epsilon=0.1$

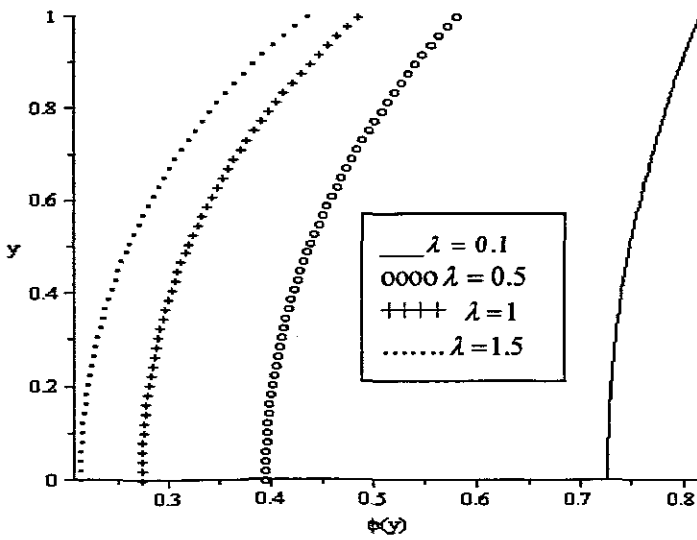


Fig.4.1.7.12. Oxygen concentration profiles for $n = 2, m=0.5, \beta=Bi=\gamma=\theta_a=1, \epsilon=0.1$

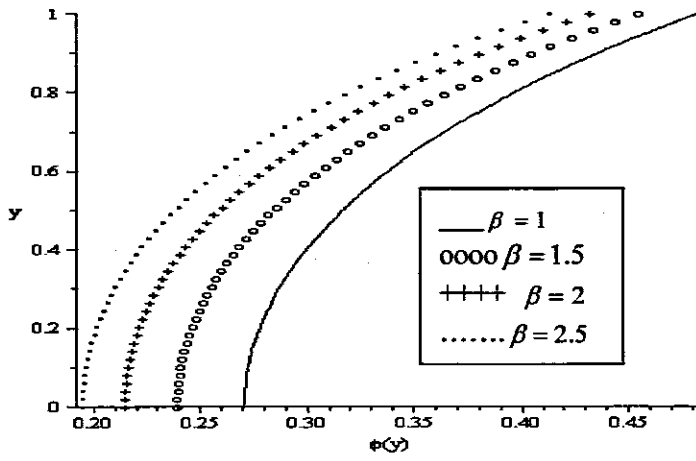


Fig.4.1.7.13. Oxygen concentration profiles for $n = 2, m=0.5, \lambda=Bi=\gamma=\theta_a=1, \varepsilon=0.1$

CONCLUSION & FURTHER WORK

5.1. CONCLUSION

We investigate in this thesis heat transfer and thermal stability in a slab subjected to Arrhenius kinetics. In chapter 3 an analysis has been carried out to study the thermal development in a combustible material under a one-step exothermic oxidation n th order chemical reaction, taking the diffusion and consumption of the reactant into account. The pre-exponential factor is assumed to be temperature dependent and the nonlinear partial differential equations governing the transient problem are solved numerically using semi-discretization technique called method of lines. The effects of various embedded parameters on the system are displayed graphically. Our results reveal among others, that the internal heat generation in the system decreases while the oxygen concentration increases with an increase in the parameter values of reaction order index (n) and Biot number (Bi). Furthermore, it is noteworthy that the slab temperature is highest while the oxygen concentration is lowest during bimolecular reaction in comparison to Arrhenius and sensitized types of chemical reaction.

In chapter 4, we considered a steady state, exothermic n th order chemical reaction in a slab with reactant consumption in the presence of convective heat and oxygen exchange with the surrounding ambient at the slab surface. The coupled nonlinear differential equations governing the system are obtained and solved using perturbation technique and together with a special type of Hermite-Padé series summation and improvement method. We validate the theoretical results using physically realistic values of various embedded parameters in the numerical experiment. A comparison between the results is obtained using the partial sum involving the first 20 terms of the perturbation series solution and purely fourth-order Runge-Kutta numerical

integration coupled with shooting method at small and moderate values of embedded parameters are shown.

As the Frank-Kamenetskii parameter (λ) increases, the slab internal heat generation due to exothermic oxidation reaction increases, this invariably leads to an elevation in the slab temperature and low concentration of oxygen. An increase in the parameter value of γ implies an increase in the supply of oxygen from the ambient to support the reaction process because oxygen supports combustion, hence is needed and very essential for this exothermic chemical reaction, leading to more internal heat been generated in the system and high temperature of the slab.

Finally the temperature can be controlled by choosing the appropriate values of embedded parameters.

5.2. FURTHER WORK

This problem was solved for a slab of combustible reactive material, hence further work can be done by considering similar problem in different geometry like cylindrical and spherical vessels.

REFERENCES

- [1] N.N. Semenov, *Some problems in Chemical kinetics and Reactivity*, Princeton University press, Princeton, (1956).
- [2] D.A. Frank-Kamenetskii, *Diffusion and Heat Transfer in Chemical kinetics*, first edition, (1955).
- [3] T. Boddington, P. Gray and C. Robinson, *Proc. R. Soc. Lond. A* 368, p. 441, (1979).
- [4] R.W.R. Muncey, *Heat Transfer Calculations for Buildings*, Applied Science Publ, London (1979).
- [5] Y. B. Zeldovich, G. I. Barenblatt, V. B. Librovich, & G. M. Makhveladze, *Mathematical Theory of Combustion and Explosion* (New York: Consultants Bureau), (1985).
- [6] L. Kuo, *Computations of Mixtures of Dirichlet Processes*, *SIAM Journal on Scientific and Statistical Computing* 7, pp. 60–71, (1986).
- [7] J. K. Dienes, *On reactive shear bands*, *Physics Letters A*, Vol. 118 (9), 433-438, (1986).
- [8] A.R. Shouman, *A very simple yet accurate solution to the thermal explosion problem*. *Journal of Loss prevention in the process Industries* 11(1998) 383-390, (1998).
- [9] Center Chemical Process Safety, *Reactive material hazards*, <http://www.aiche.org/uploadedFiles/CCPS/Resources/SafetyAlerts/reactmat.pdf>, October, 1, (2001).
- [10] S.A. El Sayed, *Thermal explosion of autocatalytic reaction*. *Journal of Loss Prevention in the process Industries* 16 249-257, (2003).
- [11] P. Gray, P.R. Lee, *Studies on criticality: Temperature profiles in explosive systems and criteria for criticality in thermal explosions*. *Symposium (International) on Combustion*, Vol. 11(1), 1123-1131, (1967).

- [12] A.G. Merzhanov, F.I. Dubovitskii and Dokl. Adad. Nauk. SSSR 120, p. 1068, (1958).
- [13] O. D. Makinde, Thermal stability of a reactive third grade fluid in a cylindrical pipe: An exploitation of Hermite-Pade approximation technique, Applied Mathematics and computation, 189 (2007) 690-697, (2007).
- [14] O. D. Makinde, Exothermic explosions in a slab: A case study of series summation technique. International Communications in Heat and Mass Transfer, Vol. 31, No.8, 1227-1231, (2004).
- [15] O.D. Makinde, Strong exothermic explosions in a cylindrical pipe: a case Study of series summation technique. Mechanical Research Communications 32(2004)191-195, (2005).
- [16] O.D. Makinde and E. Osalusi, Exothermic explosions in symmetric geometries: An exploitation of perturbation technique, vol 50; 5/6, 621-625 (2005).
- [17] F. Ferrero, C. Lohrer, B.M. Schmidt, M. Noll and M Malow, Mathematical model to predict the heating-up of large-scale wood piles, Journal of Loss Prevention in the Process Industries, 10.1016,02.09, (2009).
- [18] P. Pierre , A to Z of Thermodynamics. Oxford University Press. ISBN 0198565526, (1998).
- [19] J.M. Smith, H.C. Van Ness, and M.M. Abbot, Introduction to Chemical Engineering Thermodynamics. McGraw-Hill. ISBN 0073104450, (2005).
- [20] F.W. Sears, G. L. Salinger & J.E. Lee, Thermodynamics, Kinetic Theory, and Statistical Thermodynamics Addison-Wesley, Lebanon, Indiana, U.S.A., (1975).
- [21] R. A. Freeze, J.A. Cherry , Groundwater, Prentice-Hall, Inc., Englewood Cliffs, NJ, (1979).
- [22] J. Bebernes, D. Eberly, Mathematical problems from combustion theory. Springer-Verlag, New York, (1989).

- [23] T. R. Nunn, J. B. Howard, J. P. Longwell, W. A. Peters, Product compositions and kinetics in the rapid pyrolysis of sweet gum hardwood. *Industrial and Engineering Chemistry Process Design and Development*, 24, 836–844, (1985).
- [24] C. Lohrer, M. Schmidt, U. Krause, A study on the influence of liquid water and water vapour on the self-ignition of lignite coal – experiments and numerical simulations. *Journal of Loss Prevention in the Process Industries*, 18(3), 167–177, (2005).
- [25] Investigation Report: Chemical Manufacturing Incident, Technical Report, U.S. Chemical Safety and Hazard Investigation Board, <http://www.csb.gov/completedinvestigations/docs/MortonInvestigationReport.pdf>, (1998).
- [26] J.M. Simmie, Detailed chemical kinetic models for the combustion of hydrocarbon fuels, *Prog. Energy Combust. Sci.*, 29, 599–634, (2003).
- [27] S. Tanaka, F. Ayala, J.C. Keck, A reduced chemical kinetic model for HCCI combustion of primary reference fuels in a rapid compression machine, *Combust. Flame* 133 (2003) 467–481, (2003).
- [28] E. Balakrishnan, A. Swift, G.C. Wake, Critical values for some non-class A geometries in thermal ignition theory, *Math. Comput. Model*, 24, 1–10, (1996).
- [29] D. A. Frank Kamenetskii. *Diffusion and heat transfer in chemical kinetics*. Plenum Press, New York, (1969).
- [30] F. S. Dainton, *Chain Reaction: An introduction*, Wiley, New York, (1960).
- [31] R. Vas Bhat, J. Kuipers, G. Versteeg, Mass transfer with complex chemical reaction in gas–liquid system: two-steps reversible reactions with unit stoichiometric and kinetic orders, *Chem. Eng. J.*, 76, 127–152, (2000).
- [32] J. Warnatz, U. Maas, R. Dibble, *Combustion: Physical and chemical fundamentals, Modeling and simulation, Experiments, Pollutant formation*, Springer-Verlag Berlin and Hiedelberg GmbH and Co. K, (2001).

[33] F. A. Williams, *Combustion theory*. Second Edition, Benjamin & Cuminy publishing Inc. Menlo Park, California. (1985).

[34] M. A. Sadiq, J. H. Merkin. Combustion in a porous material with reactant consumption: the role of ambient temperature. *Mathl Comput. Modelling*, 20, 27-46, (1994).

[35] M. Berzins, J. M. Ware, Solving convection and convection-reaction problems using the method of lines. *Appl. Numerical Mathematics*, 20, 83-99, (1996).

[36] <http://en.wikipedia.org/wiki/Exothermic>